Presented at the Symposium on Statistical and
Probabilistic Problems in Metallurgy,
Seattle, Washington, August 4-6. 1971.

LBL-130
Preprint c.2

DOCUMENTS SE

THE IMPORTANCE OF GEOMETRIC STATISTICS TO DISLOCATION MOTION

Dale Klahn, Don Austin, Amiya Mukherjee,
and John E. Dorn

July 1971

AEC Contract No. W-7405-eng-48

TWO-WEEK LOAN COPY

This is a Library Circulating Copy which may be borrowed for two weeks. For a personal retention copy, call Tech. Info. Division, Ext. 5545

25

LBL-130 c.2

DISCLAIMER

This document was prepared as an account of work sponsored by the United States Government. While this document is believed to contain correct information, neither the United States Government nor any agency thereof, nor the Regents of the University of California, nor any of their employees, makes any warranty, express or implied, or assumes any legal responsibility for the accuracy, completeness, or usefulness of any information, apparatus, product, or process disclosed, or represents that its use would not infringe privately owned rights. Reference herein to any specific commercial product, process, or service by its trade name, trademark, manufacturer, or otherwise, does not necessarily constitute or imply its endorsement, recommendation, or favoring by the United States Government or any agency thereof, or the Regents of the University of California. The views and opinions of authors expressed herein do not necessarily state or reflect those of the United States Government or any agency thereof or the Regents of the University of California.

THE IMPORTANCE OF GEOMETRIC STATISTICS TO DISLOCATION MOTION

Dale Klahn,[1] Don Austin,[2] Amiya K. Mukherjee[3] and John E. Dorn[4]

July 1971

(To be presented at the Symposium on Statistical and Probabilistic Problems in Metallurgy, Seattle, Washington, August 4-6, 1971.)

1. Research Metallurgist, Inorganic Materials Research Division, Lawrence Berkeley Laboratory, Berkeley, California.

2. Computer Programmer, Mathematics and Computing Group, Lawrence Berkeley Laboratory, Berkeley, California.

3. Professor of Engineering, Dept. of Mechanical Engineering, University of California, Davis, California.

4. Professor of Materials Science and Senior Scientist respectively of the College of Engineering and Inorganic Materials Research Division of Lawrence Berkeley Laboratory, University of California, Berkeley, California.

I. Objective: Up to the present the development of dislocation theory has been the exclusive result of efforts of solid-state physicists, material scientists and metallurgists. For some time now they have recognized the serious need for introducing statistical approaches to dislocation theory so as to provide more realistic analyses for several important types of dislocation problems. As a result of their emphasis on simple approximations, however, they have attempted to treat statistically viable problems as essentially deterministic in nature, by either the adoption of smeared average approaches or by utilizing naive and somewhat questionable statistical proceedures. Whereas, the appropriate statistical content in a few simple examples was introduced into computer simulated experiments, the results of such investigations have principally served to emphasize the need for the more elegant and informative analytical formulations of the statistical aspects of these problems. What is so seriously desired is to place the "Kinetic Theory for the Motion of Dislocations" on an equally reliable statistical basis as is now enjoyed by "The Kinetic Theory of Gases." As will be shown, however, the problems of geometric statistics significant to dislocation theory are indeed much more complicated than those that have proven useful in gas dynamics.

In view of the recognized importance of dislocation theory for the understanding of the plastic behavior of crystalline materials, the acknowledged statistical nature of dislocation motion, and the stimulating statistical content of the subject, it is indeed surprising to note that mathematical statisticians have not yet contributed specifically to the development of dislocation theory. It is the objective of this paper to attempt to enlist the professional cooperation of the mathematical statistician in the

needed development of more physically realistic models for dislocation motion. To achieve this objective the authors thought it would be desirable to treat in broad terms, in preference to specific details, the following topics of interest in the subsequent sections of this report:

Section II. Historical Introduction: A short historical introduction to dislocation theory with references, to readily accessible and easily read papers, monographs, and symposia on dislocation theory for the benefit of statisticians.

Section III. Elementary dislocation concepts: A necessarily brief exposé of the minimum background in elementary geometric and dynamic characteristics of dislocations that the mathematical statistican will need in order to begin analyses on dislocation theory. As will be shown this minimum background is indeed so trivial as to be proficiently developed in a very short period of time. To reduce this discussion to tractable dimensions, however, many of the more complicated details, which are often dependent on the great versatility of dislocation behavior cannot be treated here.

Section IV. Effect of dispersed localized obstacles on the plastic yield strength of crystals. A review of three different statistical treatments of the motion of dislocations past local obstacles at zero degrees Kelvin with emphasis on the sensitivity of the analysis to the assumed statistics and methods of averaging.

Section V. Thermally activated motion of dislocations past localized obstacles. A review of steady-state motion due to thermal activation of dislocations (a) past a regular array of localized obstacles and (b) Friedel's approximation for random obstacles (c) plus analyses to be presented here for the first time on results based on simulated computerized experiments for steady-state

thermally-activated motion of dislocations past random localized obstacles. Section VI. Summary: A brief discussion on possible analytical approaches to the statistical problem of dislocation motion past dispersed localized obstacles.

II. Historical Introduction. Although a few rather incomplete concepts had been discussed in earlier reports, it is now generally agreed that the presently accepted viewpoints regarding dislocations were first announced in three papers developed independently in 1934 by Taylor[1], Orowan[2] and Polanyi[3]. These papers suggested that the then experimentally known plastic properties and slip behavior of metal single crystals required the presence and motion of line imperfections now designated to be dislocations. Whereas the existence of dislocations could be inferred indirectly by several available experimental techniques, they were first "seen" by transmission electron microscopy in 1956 by Hirsch, Horne, and Whelan[4] and independently by Bollmann[5]. It is interesting to note that some attempts to develop analytical descriptions and predictions of plastic phenomena in crystalline materials in terms of dislocation theory preceeded the development and application of transmission electron microscopy. On the other hand, both experimental and theoretical interest in dislocations was markedly stimulated by the introduction of this new experimental technique. As attested to in numerous monographs and symposia on dislocation theory[6-14], rather substantial progress has now been made in identifying many of the principles that serve to establish a firm preliminary framework for the theoretical treatment of the dynamics of dislocation motion in crystals. Despite the excellent progress that has already been made, however, much yet remains to be done not only with respect to the versatility of dislocation behavior and the large number of different types of reactions that they can undertake (vide refs. 15 and 16), but also with reference to two general problems of major importance that need be solved in order to provide more comprehensive

and realistic models for dislocation motion. These needed advances concern (a) the introduction of physically acceptable statistical approaches for more accurate rationalization of individual dislocation mechanisms and (b) the synthesis and stochastic treatment of the total effect of all possible mechanisms so as to obtain the net velocity of dislocations. A review of the rather limited progress that has been made to date on the latter topic was presented in a recent symposium (17). A brief introduction and review of the former topic will be presented in the following sections of this paper. In view of the limited space and time, the following discussion will necessarily have to be brief. For this reason the authors chose to consider only one type of dislocation mechanism, namely that of the motion of mobile glide dislocations past simple localized barriers. This selection, was made not only because of its importance to dislocation theory but also because it exposes very effectively the need for statistical approaches.

III. Elementary Dislocation Concepts: Plastic deformation in crystals is known to be the result of shear displacements of entire blocks of a crystal with respect to one another. Such shear displacements take place in specific crystallographic directions on definite crystallographic planes rather than in the direction and on the plane of the greatest resolved shear stress. The operative modes of slip directions and planes are characterized by low crystallographic indices indicating that they refer to those directions and planes that approach the highest atomic densities. The specific slip plane and direction that first responds to the applied stress as it is increased is that pair of the operative form on which the resolved shear stress is greatest. The slip response to the applied stress on parallel slip planes, however, is statistically extremely heterogeneous despite the fact that the resolved shear stress is the same on all such parallel planes. An example of such block motion is shown in Fig. 1 which refers to a slightly deformed and etched crystal of MgO. Etching causes surface pitting at points of emergence of dislocations from the body of the crystal. Obviously, after deformation dislocations are heterogeneously distributed on sets of parallel slip planes.

Glide dislocations are most easily defined as crystallographic line imperfections that demark the boundaries between slipped areas, s, and as yet unslipped areas, u, of a glide plane. The consequent topology demands that dislocations cannot terminate within the volume of a crystal but they must either form closed loops within the volume of the crystal or terminate on the crystal surfaces. The difference in slip displacement between the slipped and unslipped regions is known as the Burgers vector, b. It is usually

equal to the atomic spacing along the line of greatest atomic density in the slip plane.

Examples of slip dislocations are shown in Fig. 2.

(a) Edge Dislocation: The dislocation line, AB, is perpendicular to its Burgers vector, b, a fact which serves to define the slip plane EFF'E'. A sufficiently high shear stress τ on the slip plane in the direction of b will cause the dislocation AB to move normal to itself extending the slipped region.

(b) Screw Dislocation: Screw dislocations are distinguished from edge dislocations by the fact that the dislocation line, such as JK, is parallel to its Burger's vector. But it too will tend to move perpendicular to itself so as to extend the slipped region under sufficiently high shear stresses τ on the slip plane in the direction of its Burgers vector. Since, however, the screw dislocation line and its Burgers vector are parallel, the slip plane is not uniquely defined. If special barriers prohibit the continued motion of a screw dislocation on its original slip plane, it might, under appropriate conditions, cross-slip onto other planes that intersect the original slip plane EFF'E', along the screw dislocation JK.

(c) Curved Dislocation: The definition of a dislocation requires that the Burger vector, b, be the same along the entire length of any general curved dislocation. In the illustration of Fig. 2, segment AB of the dislocation is in edge orientation whereas segment JK of the same dislocation is in screw orientation. Along the segment from K to B the total Burgers vector can be decomposed into its edge and screw vector components b_E and b_S, respectively. Shear stresses on the slip

plane in the direction of the Burgers vector will tend to cause the dislocation to sweep over the unslipped region u by moving normal to itself.

(d) The force F acting normal to a unit length of a dislocation can be easily evaluated by applying the principle of virtual work. Eq. 1 (see Fig. 2) gives the work W, done on an edge or a screw dislocation of constant length L as it sweeps out the entire area of the slip plane. The first equality of Eq. 1 gives the work to move a dislocation in terms of the applied stress τ, the area on which it acts, and the displacement b, of the upper relative to the lower portion of the crystal. It demonstrates that the work is τb times the area swept out by the dislocation, LD. The second equality of Eq. 1 gives the work in terms of the force F, per unit length of a dislocation, times the length L, and the distance D that the dislocation is moved. As a result, the force acting on a unit length of dislocation when subjected to a stress τ is given by Eq. 2.

An atomistic picture of dislocations for the case of a simple cubic lattice is illustrated in Fig. 3. Dislocations are now seen to be line centers along which the atoms, as illustrated, are imperfectly arranged relative to their sites in the ideal crystal. Away from the central core of the dislocation lines, however, the atomic arrangement remains that for an ideal crystal excepting for small elastic displacements of the atoms from their usual relative positions in the ideal crystal. It has been convenient to describe the increase in the elastic strain energy of the crystal containing dislocations as the energy of the dislocations. The forward motion of an edge dislocation under an applied stress is depicted in the sequence of cuts (a) to (b) to (c) of Fig. 3. As the dislocation moves,

the elastic strain energy over the major volume of the crystal remains unchanged. Changes in strain energy during dislocation motion are exclusively due to changes in bond angles and relative positions of only those atoms along the core of the dislocation lines. With a few exceptions, e.g., diamonds, etc., such changes in strain energy are usually negligibly small. In this qualitative way, dislocation theory confirms the experimental observation that the plastic yield strength of face-centered cubic metallic crystals of high perfection approaches negligibly small values. As will be shown later, it also accounts for slip on a slip plane in a given crystallographic direction and for the fact that plastic yielding occurs when the resolved shear stress reaches a value that is sufficient to push dislocations past various types of barriers that they might encounter.

An understanding of the energies of dislocations is significant to an evaluation of their behavior under stresses. A detailed description of the effect of various factors that enter the quantitative evaluation of the energies of dislocations is indeed a very complicated subject. Some preliminary and useful concepts, however, are gained from a crude evaluation of the easily estimated energy of a single straight screw dislocation centered in an elastically isotropic crystal.

Figures 2b and 3d illustrate that a screw dislocation results in a spiral ramp of atoms about the dislocation core. Such a spiral ramp might be visualized to result from making an appropriately oriented radial saw cut from the surface to the center of a solid cylindrical single crystal, displacing the cut (shown in Fig. 4) by one Burger's vector b, welding the mating surfaces

of the crystal together and finally letting the cylinder relax elastically. As shown in Fig. 4, assuming the validity of Hooke's Law and elastic isotropy, the elastic strain γ_E and stress τ, are given by Eqs. 3 and 4, where G is the shear modulus of elasticity. The total line energy per unit length of the screw dislocation Γ_s of Eq. 5, arises (a) from the long range elastic strain-energy over a region from the radius of the dislocation core of about b to the outer radius R of the crystal (b) plus Γ_{SC}, the energy of the dislocation core from r = 0 to r = b. Because of the small volume of the dislocation core, the core energy is generally much less than that of the surrounding volume of the crystal despite the possibly higher energy density in the core. It can be shown that the energy per unit length of an edge dislocation where ν is Poisson's ratio is given by $\Gamma_E \approx \Gamma_S/(1-\nu) \approx 3/2\ \Gamma_S$ which is only slightly greater than that for a screw dislocation. Whereas, the energies of dislocations in isotropic media increase linearly with G, they are not fixed quantities but depend not only on the crystal diameter, but also whether the dislocation is in screw or edge orientation. Furthermore, the energy of curved dislocations decrease, due to elastic interactions between the various segments of curved dislocation, as their radius of curvature decreases. The energy of dislocations also decrease in the proximity of dislocations of opposite signs (vide Fig. 3e). For the following analyses the authors will adopt the convenient approximation that the line energy per unit length of a dislocation has the substantially constant value of Γ regardless of elastic anisotropy of the crystal orientation of the dislocation line, its radius of curvature, crystal size, surface effects, and small changes in the sign and density of surrounding dislocations.

As previously mentioned, dislocations in almost perfect crystals of face-centered cubic metals begin to move under vanishingly small applied stresses. Obviously, viscous drag and lattice friction effects must be extremely small in these cases. Much higher stresses, however, are required to make dislocations move in other less perfect, alloyed metal crystals of the same base metals. Such effects must arise from the presence of obstacles to the motion of dislocations. Although various types of obstacles have been identified (15, 16) it will not be possible to describe the various classes and their unique effects, in this report. For the present objective, it will be sufficient to consider only the presence of local obstacles to the motion of a dislocation. Under small applied stresses τ, the forward motion of a dislocation when it contacts the local obstacles as shown at points P_1 and P_2 of Fig. 5. The line energy of a dislocation is proportional to its length ℓ as given by Eq. 9. Hence, a dislocation arc attempts to assume its minimum length. Consequently, the force along the length of the dislocation, or line tension, is given by Eq. 10. Any small arc $Rd\theta$ of the dislocation line between the obstacles is acted upon by two forces. The first term of Eq. 11 is the force τb per unit length of dislocation times the length $Rd\theta$ acting normal to the dislocation line as a result of the applied stress. The second term of Eq. 11 is the force on the dislocation line due to the line tension. Under mechanical equilibrium these terms are identical, revealing that the radius of curvature of the entire dislocation arc is given by the constant value $R = \Gamma/b\tau$ for the case of constancy of Γ assumed here.

The various types of localized obstacles such as the strain fields of solute atoms, the presence of coherent precipitates, intersections of repulsive

dislocations, etc., each exhibit unique force-displacement, F-x, diagrams for the cutting of the obstacles. For the analyses to be done here the simple rectangular F-x diagram shown in Fig. 6 which is believed to approximate that for the "cutting" of forest dislocations threading the slip planes by glide dislocations moving in the slip planes, will be used. When a resolved shear stress is applied, the dislocation contacts obstacles P_1, P_2, and P_3, in Fig. 6a, and bows out into circular arcs. The radius of curvature of these arcs is given by Eq. 12 (See Fig. 5). As the applied shear stress is increased, the radius of curvature of the arcs decreases and hence the angle ψ, included between the two arms of the bowed out dislocation at P_2, decreases. Ultimately, at some critical value of the angle ψ_c, the force on the obstacle is just sufficient to overcome the strength of the obstacle. Thus $2\Gamma \cos \psi_c/2$ is a measure of the strength of an obstacle in terms of the line energy of a dislocation. This critical force is given by F_C in Eq. 13 and the corresponding obstacle force-displacement diagram is shown in Fig. 6b, where d is the obstacle-dislocation interaction distance. The resultant work done (Eq. 14) for mechanically cutting the obstacle is shown by the shaded region in Fig. 6b and is equal to $2\Gamma d \cos \psi_c/2$.

Figure 7 shows an actual example of dislocations in MgO bowing under stress between small precipitates, which are believed to be magnesium nitride[13].

IV. Effect of Dispersed Localized Obstacles On The Plastic Yield Strength of Crystals: The yield stress is frequently defined as that stress at which small prescribed plastic strains are first obtained. In the present context it will be convenient to associate such yielding with the stress necessary to cause a dislocation to traverse an entire slip plane. Whereas at higher temperatures, thermal fluctuations can assist the stress work needed to cut obstacles, at $0^{\circ}K$ all of the work must be done mechanically. In this section three alternate estimates will be made of the stress necessary to mechanically force a dislocation to traverse a slip plane at $0^{\circ}K$:

(a) In the first estimate the obstacles will be assumed to be distributed in a square array on the slip plane.

(b) A more realistic distribution of randomly positioned obstacles will be assumed in the second approximation. However, in lieu of a complete statistical consideration of the problem, the analysis will be based on Friedel's (19) approximation.

(c) Finally results, accurate to within the limitations of the assumptions made, obtained by the computer simulated experiments of Foreman and Makin (20,21) will be compared with the more approximate analyses.

The results of all three examples will be expressed in terms of L_s^2, the average area of the slip plane occupied by an obstacle, and the obstacle strength as given by $F_c = 2\Gamma \cos \psi_c/2$.

(a) Regular array: As shown in Fig. 8 the smallest uniform distance between the obstacles in a square array is L_s. Consequently, as shown by Eq. 15, the force needed to cut one obstacle is given by $F_c = 2\Gamma \cos \psi_c/2 = \tau_0 b L_s$ where the subscript zero refers to the absolute zero of temperature.

(b) Friedel approximation: The simplifying assumption that localized

obstacles form a regular square array is seldom valid. Occasionally they are clustered as in cold-worked metals, where the forest dislocations are mostly concentrated in the entanglements comprising the cell walls. Usually they are more or less randomly distributed as in the case of solute atom strain fields and radiation-induced strain centers.

Friedel(19) was first to introduce elementary concepts of statistics to the motion of dislocation past randomly distributed point obstacles. As the applied stress is decreased the radius of curvature of the bowed-out arcs of dislocation arrested at local obstacle increases. Consequently the average cord distance, ℓ, between adjacent obstacles subtended by a dislocation arc increases as the stress decreases. Friedel attempted to estimate the influence of this effect on the yield stress by assuming that the average configuration might be approximated as shown in Fig. 9. He assumed that when the stress became high enough to cause the dislocation to cut the obstacles at A, B, C etc., the dislocation advanced to the next set of obstacles eg., B' etc., where the area swept out per obstacle, L_s^2, is approximated by Eq. 16. As required by the simple geometric relationship of Eq. 17, for weak obstacles, where $h \ll 2R$, the mean cord length between adjacent weak obstacles decreases with increasing values of the applied stress as approximated by Eq. 18. Accordingly, following Eq. 19, the flow stress τ_o at the absolute zero corresponding to a critical value of the included angle ϕ_c, is given by

$$\frac{\tau_c L_s b}{2\Gamma} = (\cos \phi_c/2)^{3/2} \qquad \text{Eq. 19a}$$

This relationship is shown by the finely dashed line in Fig. 10 where it is compared with that given earlier for a regular square array. Obviously

the yield stress is highly sensitive to the distribution of obstacles, being lower for the random arrangement when compared to the square array of the same obstacles, the differences become most marked for very weak obstacles ($\psi \rightarrow 180^{\circ}$). This comparison reveals the importance that must be ascribed to a consideration of the statistics of the problem. since the yield stress for randomly distributed weak obstacles is many times less than that calculated for a square array.

(c) Computer simulated experiments of Foreman and Makin: Because of its inherent complexity no exact analytical formulation for the statistical treatment of a dislocation moving through a random array of local obstacles has yet been presented. On the otherhand, Foreman and Makin (20,21) have shown that it is possible to obtain an accurate solution to this problem by means of a computer simulated experiment. Their approach consisted of laying down 10,000 computer selected randomly positioned obstacles on a slip plane. (This gave results that were within 5% of that given for a random array consisting of 1,000 points only.) A dislocation line was considered to start at the bottom of the slip plane. In order to account more accurately for the side boundary effects, the obstacles on either side were considered to be positioned at mirror images of those on the operative slip plane. When a small stress was applied the dislocation contacted and bowed out between adjacent obstacles. The program was so written as to permit the dislocation to "cut" and therefore pass all initially contacted obstacles at which ψ was less than ψ_c. Finally, under the small initial stress, the dislocation became arrested along its entire length when ψ was greater than ψ_c at all contacted obstacles. Under these conditions a slightly

higher stress was applied, etc., until the yield stress, at which the dislocation swept over the entire slip plane, was reached. A "best fit" of their yield stress data is shown in Fig. 10. A convenient empirical expression which quite accurately duplicates Foreman and Makins' data was found to be

$$\tau_o L_s b/2\Gamma = \left(\frac{\cos \psi_c/2}{1.096}\right)^{1/.69} \tag{19b}$$

This relationship is also shown in Fig. 10.

Whereas Foreman and Makins' theoretically more acceptable results fall somewhat below the curve for a square array and Friedel's approximation for strong obstacles, the agreement with Friedel's approximation over the range of weak obstacles is reasonably good.

The analysis showed further that the characteristics of the dislocation movement changed substantially with the angle, ψ_c. When this angle is small (strong obstacles), the dislocation line had a tendency to penetrate the array deeply along path of easy movement, where the obstacles were far apart, often encircling groups of more closely spaced obstacles and thus leaving closed loops behind. When the angle was weak ($\psi_c \simeq \pi$), the low value of the stress caused the dislocation to remain relatively straight as it moved through the array and consequently few loops were formed. In addition, for stresses approaching the yield stress, τ_o, cutting at one obstacle would often result in cutting at adjacent obstacles when their included angles became less than or equal to ψ_c. This phenomena is known as "unzipping."

V. Thermally Activated Motion of Dislocations Past Localized Obstacles: Whereas, as discussed in Sec. IV, at $0^{\circ}K$ dislocations can only be forced past obstacles by direct mechanical action due to the applied stress, at all higher temperatures part of the work needed to cut localized obstacles is also supplied by thermal fluctuations in energy. The frequency of thermal fluctuations is usually expressed in terms of transition-state reaction kinetics, as examplified by Eyring's reaction rate theory (22), according to which

$$\nu' = \nu \exp - g/kT \tag{21}$$

where ν is an attempt frequency and kT has its usual significance of the Boltzmann constant times the absolute temperature. The term g refers to the additional isothermal and constant pressure work that need be supplied by a thermal fluctuation in order to cut the obstacle. Accordingly, g is known to be the Gibbsian free energy for activation. The evaluation of g for the simple rectangular F-x diagram for cutting that was adopted here is shown in Fig. 11. Under an applied stress $\tau < \tau_o$ the dislocation bows on either side of an obstacle to subtend the angle $\psi > \psi_c$ so that the dislocation becomes momentarily arrested. After a period of time, to be determined later, a fluctuation in free energy results in cutting the obstacle. The work of cutting done by the applied stress is merely $2\Gamma d\cos\psi/2$ and the total work of cutting need be $2\Gamma d\cos\psi_c/2$. Therefore, g, as given by Eq. 21, must equal, or be greater than, the cross-hatched area of Fig. 11.

For the simple string model that is being considered here it has been suggested by Friedel that the attempt frequency might be approximated by the lowest vibrational mode of the dislocation, namely $\nu = \nu_o b/\lambda$ where ν_o

is the Debye frequency. Granato, Lucke, Schlipf, and Teutonico (23), have shown that somewhat higher attempt frequencies are often appropriate; furthermore, Lothe (24) has submitted additional alternate arguments for this viewpoint. Since the frequency of activation depends exponentially on the free energy for activation and only linearly on the attempt frequency it will not introduce significant error to the proposed analysis to assume ν to be constant.

In terms of the previous discussion, even when the applied stress is less than that needed for yielding at $0^{\circ}K$, the dislocation can yet cut obstacles by the aid of thermal fluctuations. Since ν' is the average frequency for a successful thermal fluctuation, the motion of the dislocation is arrested at each obstacle for the time $t=1/\nu'$ for cases where $\cos\psi/2$ remains constant. After this interval of time, the dislocation cuts the obstacles and moves forward to a new advanced position. The frequency for the reverse activation, i.e., for motion in the opposite direction against the stress, is so small that it can be neglected. Furthermore the inertia of dislocations is so small that times devoted to their acceleration, free flight, and stoppage at the next obstacle can, to a good approximation, be neglected relative to their wait time for thermal activation (17).

Since thermally activated motion of dislocations is time dependent it is convenient to express the results in terms of the velocity of dislocations as determined by the applied stress (now designated as the flow stress), the temperature, and the obstacle strengths and their distributions. In the following paragraphs of this section three different types of analyses will be outlined, namely, (a) that for a regular square array of obstacles, (b) that for Friedel's approximation for randomly distributed obstacles and

(c) newly obtained data, presented here for the first time, on computer simulated experiments for thermally activated motion of dislocations past randomly distributed obstacles.

(a) Regular Square Array: As shown by Fig. 8 for the square array the dislocation advances as a unit a distance L_s in the period of a single thermal fluctuation. Therefore, the average velocity of the dislocations in a regular square array, designated by subscripts s, is given by

$$v_s = \nu L_s \exp - \frac{2\Gamma d}{kT} (\cos\psi_c/_2 - \cos\psi/_2)$$

$$v_s = \nu L_s \exp - \frac{2\Gamma d}{kT} (\cos\psi_c/_2 - \tau_s L_s b/_{2\Gamma}) \qquad (22)$$

where the second equality follows from Fig. 8.

(b) Friedel's Approximation. As shown in Fig. 9, the dislocation advances, on the average, a distance h for each successful thermal fluctuation for the Friedel steady-state approximation. Therefore, using subscripts F to designate Friedel's approximation

$$v_F = \nu h \exp - \frac{2\Gamma d}{kT} (\cos \psi_c/2 - \cos \psi/2)$$

$$v_F = \nu L_s \left(\frac{\tau_F L_s b}{2\Gamma}\right)^{1/3} \exp - \frac{2\Gamma d}{kT} \{\cos \psi_c/2 - (\tau_F L_s b/_{2\Gamma})^{2/3}\} \qquad (23)$$

where the second equality follows from the introduction of Eqs. 19 and 20.

The significant differences in the calculated velocities of dislocations for the cases of regular square arrays and for Friedel's approximation for a random distribution of obstacles is seen directly from Eqs. 22 and 23. At $T = 0^oK$ the results agree with those documented in Fig. 10. Whereas the τ_s vs T relationship is linear at constant dislocation velocity and τ_s decreases to $\tau_s = 0$ for the critical temperature given by $kT_c/2\Gamma d = (\cos \psi_c/2)/(\ln L_s \nu/v_s)$.

Except for $\cos \psi_c/2 \approx 1$, τ_F is substantially lower than τ_s at $0^\circ K$, especially for weak obstacles and decreases at first more rapidly than τ_s with increasing temperatures. (In contrast to τ_s, which is zero for all temperatures above T_c, τ_F finally becomes asymptotic to zero for constant values of the dislocation velocity.)

(c) Computer Simulated Experiments on Thermally Activated Motion of Dislocations. Preliminary data on the thermally activated motion of dislocations past localized obstacles, as deduced from computer simulated experiments, have become available recently. These data will be presented here for the first time in brief outline form; more extensive and detailed coverage of this subject will be the basis for a more comprehensive future study and report.

Several interesting details of the thermally activated cutting of localized obstacles by the dislocation are lucidly exposed in these computer simulated experiments. Furthermore, within the limits of the simplifying assumptions that were adopted, the computerized experiments present what is believed to be an accurate statistical representation of the results that are obtained, neglecting, of course, interactions between various glide dislocations that might be present in a real case as well as complications arising from the operation other possible velocity controlling mechanisms. Thus, these data not only provide a guide for formulating an analytical approach to the statistical treatment of the subject but also give the simulated computerized experimental data for checking the accuracy of analytical approximations that might be designed for the solution of this problem in the future.

Analyses were conducted on a CDC 6600 digital computer. The computer was programmed to lay down initially 999 randomly distributed point obstacles, of the type under discussion, on a square area. A dislocation line was initially positioned at the bottom of the square slip plane area. In order to obtain reasonable boundary conditions at the sides of the selected slip plane area, the original random pattern of obstacles was reflected across each side boundary in a manner identical with that adopted by Foreman and Makin. Thus all dislocation arcs at the two side boundaries of the slip plane always acquired a zero slope. In order to determine the steady-state velocity of the dislocation, each computerized experiment was conducted holding the stress as well as the obstacle strength and temperature constant. The range of physically interesting stresses, obstacle strengths, temperatures, and velocities which were investigated are shown in Table 1. Also shown in Table 1. are the nondimensional forms of the various parameters which were used in this analysis.

When the constant stress $\tau < \tau_o$ was applied, the dislocation was programmed to bow out between the obstacles to its constant radius of curvature, $R = \Gamma/\tau b$. If the angle ψ between the two branches of the dislocation that contact an obstacle were less than ψ_c, the program permitted the dislocation to cut and pass the obstacle without delay. For obstacles at which ψ was greater than ψ_c, however, it was demanded that the dislocation remain arrested at that point for the time interval needed to assure thermal activation past that obstacle. For each new configuration of the dislocation as it swept across the slip plane,

TABLE I

PARAMETER	SYMBOL	NONDIMENSIONAL FORM	RANGE
length	ℓ	ℓ/L_s	------
area	A	A/L_s^2	------
time	t	νt	------
velocity	v	$v/L_s\nu$	$10^{-5} - 10^{-20}$
stress	τ	$\tau L_s b/2\Gamma$	$0.2\tau_o - 0.8\tau_o$
temperature	T	$2\Gamma d/kT$	as needed
obstacle strength (relative)	$\cos \psi_c/2$	----------	.9,.675,.45,.325

where,

L_s^2 = average area per obstacle

ν = attempt frequency (constant)

Γ = line tension (constant)

d = width of rectangular force - displacement diagram

k = Boltzmann constant

τ_o = absolute zero flow stress

the remaining wait-time for a successful thermal fluctuation was determined for each obstacle contacted by the dislocation line. Thus the next obstacle to be cut by the dislocation could be identified as that for which the remaining time of wait was the least. Each time one obstacle was cut the value of ψ, for the two adjacent obstacles, changed. Adjacent obstacles, at which the ψ values became less than ψ_c, were cut without additional delay as demanded by the program design. Dependent on the obstacle strengths and applied stresses, a series of adjacent obstacles would frequently be "unzipped" following some thermally activated cuttings. After determining the new dislocation position the residual times of wait for all obstacles contacted by the dislocation were redetermined to identify that obstacle among those now contacted which would be first cut.

The determination of the residual time for thermally activated cutting of an obstacle was based on the appropriate extrapolation of Eq. 21 for the case where $g = 2\Gamma d\ (\cos\psi_c/2 - \cos\psi/2)$ is a function of time, since $\cos\psi/2$ might decrease with time. The previously adopted deterministic interpretation of Eq. 21 is retained for this extrapolation so that the total wait time t, following contact between the dislocation and an obstacle at t = o, for a successful thermal fluctuation is given by,

$$1 = \int_0^t \nu \exp\frac{-2\Gamma d}{kT}(\cos\psi_c/2 - \cos\psi/2)dt \qquad \text{Eq. (24)}$$

For cases where $\cos\psi/_2$ remains constant this expression reduces to the simple case given by Eq. 21, where $\nu' = 1/t$.

A more convenient form of Eq. (24) can readily be formulated so as to permit direct evaluation of the residual wait times for all obstacles contacted by a dislocation line. Consider the time at which the jth activation has just been completed. The dislocation will then have cut by thermal activation j obstacles and may have cut additional obstacles by "unzipping". Assume that the pth obstacle now on the dislocation was first contacted at the ith activation where i<j. Therefore, for each obstacle p on the dislocation line, according to Eq. 24,

$$1 = \sum_{n=i+1}^{n=j+1} \nu(\Delta t)_{p,n} \exp\frac{2\Gamma d}{kT}(\cos\psi_c/2 - \cos\psi_{p,n}/2) \qquad \text{Eq. (25)}$$

Eq. 25 gives the residual wait times, $(\Delta t)_{p,j+1}$ for each obstacle p on the dislocation line from which the minimum value can be determined and that obstacle cut by the dislocation can be identified. In this manner the dislocation moves in a point by point fashion through the array. As the dislocation approaches the top of the array the experiment is terminated. During the dislocation motion the area swept out by the dislocation and the total elapsed time are tabulated as shown in Fig. 12. The average dislocation velocity is taken to be the slope of the area vs. time data divided by the projected dislocation length.

Initially twelve different randomly selected arrays of 999 obstacles each were examined to ascertain whether this number of obstacles was sufficient to provide representative average results. The criterion of the average dislocation velocity was employed for this evaluation.

Preliminary results showed that the variations in dislocation velocities among the series of twelve random distributions of obstacles that were examined became embarrassingly significant for low values of the

stress and also for high values of the stress, especially at high obstacle strengths. For values of $\tau L_s b/2\Gamma$ less than 0.05 the radius of curvature of the dislocation became so large that in some regions the dislocation subtended only a few obstacles within the slip plane area. Under these conditions many more than the selected 999 obstacles are required to obtain a good sampling. Consequently for the data reported here only stresses above $\tau L_s b/2\Gamma = 0.05$ were investigated, although the variance in dislocation velocities was large over all conditions tested especially at high stresses, $\tau L_s b/2\Gamma$, and at high obstacle strengths, $\cos \psi_c/2$, it was not deemed to be excessive.

In order to provide a reasonably accurate and common basis for comparing the effect of the various factors, that specific array among the twelve was selected for detailed evaluation which gave about the mean dislocation velocity for the rather stringent conditions of $\cos \psi_c/2 = 0.9$ and $\tau/\tau_o = 0.8$. Therefore the data reported here, although they may be of somewhat questionable absolute accuracy, nevertheless should provide reasonably good internal consistency regarding the effects of obstacle strengths, stress, and temperature on the dislocation velocity since all reported data refer to one somewhat average random array of obstacles.

When the stress is first applied, the dislocation advances instantaneously so as to contact a series of obstacles in "zero" time. In contrast, during the following stages of steady-state thermally activated motion of the dislocation, each obstacle is contacted

at different times. This suggested that in order to provide for the appropriate steady-state initial conditions, the dislocation must be permitted to advance past the first set of contacted obstacles before any accurate evaluation of the dislocation velocity in terms of elapsed time and area swept out might be made. It was found, however, that the dislocation velocities calculated without correction scattered on either side of those for which corrections for the initial conditions were made. It appears that in large measure this observation might be attributed to variation in the velocity of the dislocation as it travels over the slip plane; evidently this variation is greater than the effects of the initial conditions. Undoubtedly this anomaly could be resolved by employing a much greater number of obstacles. For the present intent, however, it was considered not to be too serious to neglect corrections for initial conditions.

The Vista System of the CDC 6600 computer permitted direct viewing of the dislocation moving by thermal activation through a forest of obstacles. Several interesting features of thermally activated dislocation motion were recorded in a movie which is described in the appendix of this report. The Vista System was also extremely helpful in formulating and "debugging" this program.

Over regions where obstacles were greater than the average distance apart the dislocation speeded up and it slowed down where the density of obstacles was higher than average. For strong obstacles ($\cos \phi_c/2 \approx 1$)

and high applied stresses ($\tau/\tau_o > .8$) the dislocation would tend to encircle regions more densely populated with obstacles and the positive and negative branches of the encircling dislocation would annihilate each other leaving a closed dislocation loop behind. Such dislocation loops eventually disappeared due to thermal activation and self annihilation. Fig. 13 shows a dislocation in the early stages of motion through a random array from which a closed loop has been left behind. The dark triangle in Fig. 13 (at an obstacle on the loop) denotes that obstacle which is going to be cut next by thermal activation. To aid in debugging the program and to follow the history of each obstacle during the motion of the dislocation over the slip plane, their vertical coordinates were usually programmed to reduce to zero regardless of whether they were cut as a result of thermal activation or unzipping. The program was thus observed to be faulty whenever isolated obstacle points that were not encircled by a closed dislocation loop were left on the traversed slip plane.

A hasty guess might suggest that the sequence of cutting obstacles in a given random distribution should be independent of the temperature. As shown in Fig. 14, however, this guess is incorrect. Two dislocations are shown in each of six sequential frames. The thermally activated motion of both dislocations were studied at $\tau/\tau_o = 0.4$ for obstacle strengths designated by $\psi_c = 95°$. The dislocation shown by the solid line underwent thermally activated motion at $2\tau d/kT = 50$ whereas that represented by the dotted line was activated at a higher temperature (or a correspondingly lower value of τd) designated by $2\tau d/kT = 1$.

The triangle below the dislocation lines identified that point at which cutting of an obstacle will occur next. Over frames 1 to 4 the same obstacle is next cut independent of temperature differences. But in frame 5, the triangle to the left identifies the point that would next be activated at $2\Gamma d/kT = 50$ whereas the triangle to the right illustrates that a different point would be activated next at $2\Gamma d/kT = 1$. In frame 6 the next points to be activated are also seen to depend on $2\Gamma d/kT$. The variation of the sequence with which obstacles were cut was common to all of the computer simulated experiments on thermally activated motion of dislocations that were conducted.

For the purpose of future analyses, the unzipping ratio, u, given by the fraction of obstacles that were unzipped was also determined. As shown in Fig. 15 the unzipping ratio was independent of the temperature, decreased with increasing obstacle strength, and varied in a sigmoidal fashion from 0 to 1 as τ/τ_o increased from 0 to 1. It is important to recognize, however, that except for u approaching 1 as τ/τ_o approached 1, the dislocation remained arrested for a period of time at the obstacle before it was unzipped.

For the obstacle strength of $\cos \psi_c/2 = 0.675$, dislocation velocities are given in Fig. 16 in terms of $\ln (v/L_s\nu)$ as a function of the reduced temperature $2\Gamma d/kT$ for each of a series of stresses represented in dimensionless form by $\tau L_s b/2\Gamma$. Similar trends were obtained for all other obstacle strengths that were investigated insofar as the logarithm of the dislocation velocity decreased almost linearly with

the reciprocal of the temperature for each constant value of the stress. Although the theoretical justification of the following formulation has not been established, the data agree well over the full range of conditions that were investigated with Eq. 26,

$$v/L_s\nu = c(\tau L_s b/2\Gamma)^m(1/1-u)\exp - \frac{2\Gamma d}{kT}\{\cos\psi_c/2 - f\,(\tau L_s b/2\Gamma)^n\} \quad \text{Eq. (26)}$$

where

c = constant ≈ 6.9

m = constant ≈ .63

u = unzipping ratio

For the range of conditions that were examined, f and n seem to be dependent only on the obstacle strength and then only mildly so as shown in Figs. 17 and 18, respectively.

The yield stress at 0°K can be deduced from the computer simulated experiments on thermally activated cutting of obstacles with a dislocation by demanding that the numerator of the term in the exponent of Eq. (26) be zero. Consequently

$$\frac{\tau_o L_s b}{2\Gamma} = \left(\frac{\cos\psi_c/2}{f}\right)^{1/n} \quad \text{Eq. (27)}$$

The datum points obtained with this approach are shown by triangles in Fig. 10. The fact that these results are in very good agreement with those obtained previously by the alternate and more direct procedure adopted by Foreman and Makin also shown in Fig. 10, serves to strengthen

confidence in the nominal validity of the approach that was used to determine the thermally activated motion of dislocations past localized obstacles. In addition it should be observed that the form of Eq. (27) is identical to the empirically derived fit of the Foreman and Makin data given by Eq. (19b).

In order to correlate the computer simulated analyses it will prove convenient to define a critical temperature, T_c, as that which will result in a selected dislocation velocity, v, when the applied stress term of the exponential is zero. Accordingly

$$\frac{2\Gamma d}{kT_c} = \frac{\ln\left\{\left(\frac{\nu L_s}{v}\right) c\left(\frac{\tau L_s b}{2\Gamma}\right)^m \left(\frac{1}{1-u}\right)\right\}}{\cos \psi_c/2} \qquad \text{Eq. (28)}$$

Introducing this value for $2\Gamma d/kT_c \cos \psi_c/2$ permits Eq. (26) to be rewritten in the convenient form

$$\left(\frac{\tau}{\tau_o}\right)^n = \left(1 - \frac{T}{T_c}\right) \qquad \text{(Eq. (29)}$$

All of the data obtained from the computer simulated experiments for the series of obstacle strengths that were investigated are summarized in terms of τ/τ_o vs. T/T_c in Fig. 19. Although τ_o and T_c increase linearly with $\cos \psi_c/2$, the reduced relationships given in Fig. 19 illustrates that τ/τ_o for the higher obstacle strengths lies only slightly above those for the lower strengths at intermediate values of T/T_c. The fact that Friedel's approximation agrees well with the

$\cos \psi_c/2 = 0.675$ constitutes a tribute to his remarkable physical insight.

VI. Discussion: No apologies will be presented for utilizing the rather naive and simplistic approximations for dislocation structure of crystals and for the dynamics of dislocation motion that were employed in the preceding sections of this report. Furthermore, no excuses will be offered for the omission of extensive additional knowledge on dislocation theory that is relevant to the objective of this paper. The authors' major thrust concerned the indoctrination of mathematical statisticians in a few of the most elementary aspects of dislocation theory in order to illustrate the need for their professional expertise for the essential future development of dislocation theory within the needed statistical framework.

Although more accurate numerical results could have been obtained for the line energy model of a dislocation by taking into consideration (a) elastic anisotropy, (b) possible dislocation dissociation and stacking fault energy, (c) the curvature of dislocations and interactions between branches of the same dislocation, (d) the differences due to orientation and the magnitude of edge and screw components, such second order corrections, as given in a recent publication (25), would have constituted diversions that would not have altered the major analytical principles that were presented.

The limitations of the preceding analyses to the singular example where the barriers to the motion of a dislocation are exclusively simple localized obstacles presents a very restrictive hypothetical case. In actuality many types of dislocation interactions are known to occur. At low temperatures (15,17) several types each of athermal, thermally activatable and dislocation

drag mechanisms are operative at one time. The actual dynamics of dislocation behavior therefore depends on the net effect of the simultaneous interaction of all such operative mechanisms. A rational and satisfactory statistical approach to the synthesis of a series of mechanism is yet very incomplete and should prove to present a worthy challenge to the mathematical statisticians. Improved analytical approaches to the simple case of dislocations cutting a distribution of localized point obstacles, which was discussed in the previous sections of this report might serve to uncover appropriate treatments for the more realistic cases.

A comparison of the results that are predicted when localized obstacles are distributed in a square array with those given by Friedel's approximation for randomly distributed obstacles, serves to emphasize the significance of the assumed distribution of obstacles as well as the great effect on the results obtained by using statistical methods. On the other hand it is indeed surprising that Friedel's approximate results agree so well with those obtained by computer simulated experiments. There seems to be as yet only incomplete statistical justification for the assumed geometry of Fig. 9, where the contacted obstacles are on an originally straight dislocation line each an equal average cord distance ℓ apart and that the average area swept out per activation is always equal to the average area occupied by one obstacle. Furthermore Friedel's approach completely neglects possible effects of unzipping on the average dislocation velocity.

Somewhat improved statistical treatments for estimating the yield stress at 0°K have been proposed by Kocks (26-30). For a random distribution of

point obstacles Kocks correctly expressed the probability, dp, of finding an obstacle in element of area dA in terms of the area previously swept out by the dislocation without contacting an obstacle as

$$dp = e^{-A/L_s^2} \frac{dA}{L_s^2} \qquad \text{Eq. (30)}$$

He employed computerized experiments for the yield stress to justify the somewhat arbitrary conditions that he employed. Furthermore he also estimated the probability of unzipping in terms of the probability of passage of dislocations through cords joining obstacles. Although some of the statistical concepts that he has employed are empirical and cannot be fully justified theoretically, nevertheless Kocks has opened the way for more rational statistical treatments of the yield stress.

Computer simulated experiments on the motion of dislocations through a forest of localized obstacles can easily be programmed so as to include accurately the complete statistical content of the problem. The results of such analyses represent the most reliable data currently available. Furthermore the computer simulated experiments are invaluable for identifying the various details of dislocation motion that have statistical significance. As utilized by Kocks, they can serve as empirical guides to the formulation of reasonable statistical approximations. On the other hand it is often more informative and useful to use completely analytical approaches to the statistical problems. These need yet be more accurately developed.

Before the motion of a dislocation can be formulated in terms of the net effect arising from a statistically reliable synthesis of the simultaneous

operation of all viable dislocation mechanisms, it will first be necessary to answer the much simpler question regarding the motion of a dislocation through a spatial distribution of obstacles that have a spectrum of strengths. Foreman and Makin have already determined by computer simulated experiments how the yield stress at 0°K varies as the relative concentrations of two strengths of obstacles are changed. Approximate analytical treatment of these examples by Kocks (29) gave analogous results.

An approximate treatment for the thermally activated motion of a dislocation past a square array of obstacles having a random spectrum of strengths was presented by Frank (31,32). More recently a treatment of thermally activated dislocation motion past randomly positioned obstacles having a spectrum of activation energies was presented by Labusch (33). Several questions concerning the statistical formulation of these approaches have been posed by Kocks (30). Whereas both represent some progress in approaching the full statistical treatment for thermally activated motion of dislocations past localized obstacles, neither has attempted a completely rigorous formulation of the problem.

Acknowledgement

This research was conducted as part of the activities of the Inorganic Materials Research Division of the Lawrence Radiation Laboratory of the University of California, Berkeley, and was done under the auspices of the U. S. Atomic Energy Commission.

List of Figure Captions

Fig. 1. Dislocation etch pits in slip bands of plastically deformed single crystal of MgO. Four sides of square crossectional area specimen are shown side by side.

Fig. 2. Glide dislocations.

Fig. 3. Atomistic representation of dislocations.

Fig. 4. Strain energy of a screw dislocation.

Fig. 5. Radius of curvature of a dislocation.

Fig. 6. Cutting of point obstacles.

Fig. 7. Bowing out of pinned dislocation in MgO.

Fig. 8. Square array analysis.

Fig. 9. Friedel's analysis.

Fig. 10. Yield stress at $0^{\circ}K$ vs. obstacle strength.

Fig. 11. Rectangular force-displacement diagram.

Fig. 12. Area swept out by glide dislocation vs. elapsed time.

Fig. 13. Glide dislocation moving through random array of point obstacles. Closed loop left behind. Next activation at dark triangle on loop.

Fig. 14. Sequence of activation for two dislocations at different values of $2\Gamma d/kT$. For solid dislocation line $2\Gamma d/kT = 50$; for dotted dislocation $2\Gamma d/kT = 1$.

Fig. 15. Fraction of obstacles unzipped vs. obstacle strength and applied stress.

Fig. 16. Results of computer experiments for $\cos \psi_c/2 = .675$. showing average dislocation velocity vs. $2\Gamma d/kT$ for a series of stress levels.

Fig. 17. Values of parameter f (see Eq. 26) for four obstacle strengths.

Fig. 18. Values of parameter n (see Eq. 26) for four obstacle strengths.

Fig. 19. τ/τ_c vs. T/T_c for four obstacle strengths.

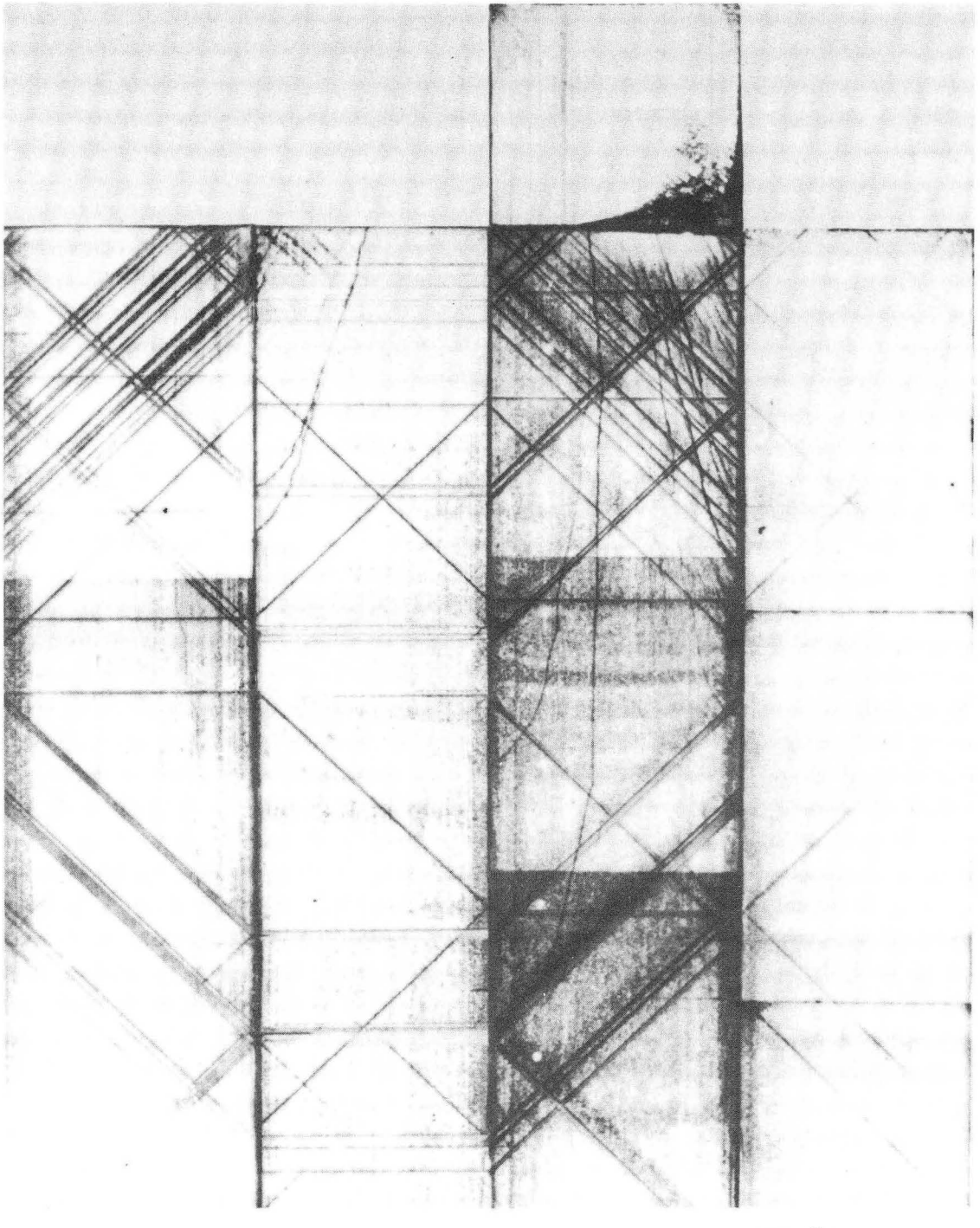

IM-649

Fig. 1

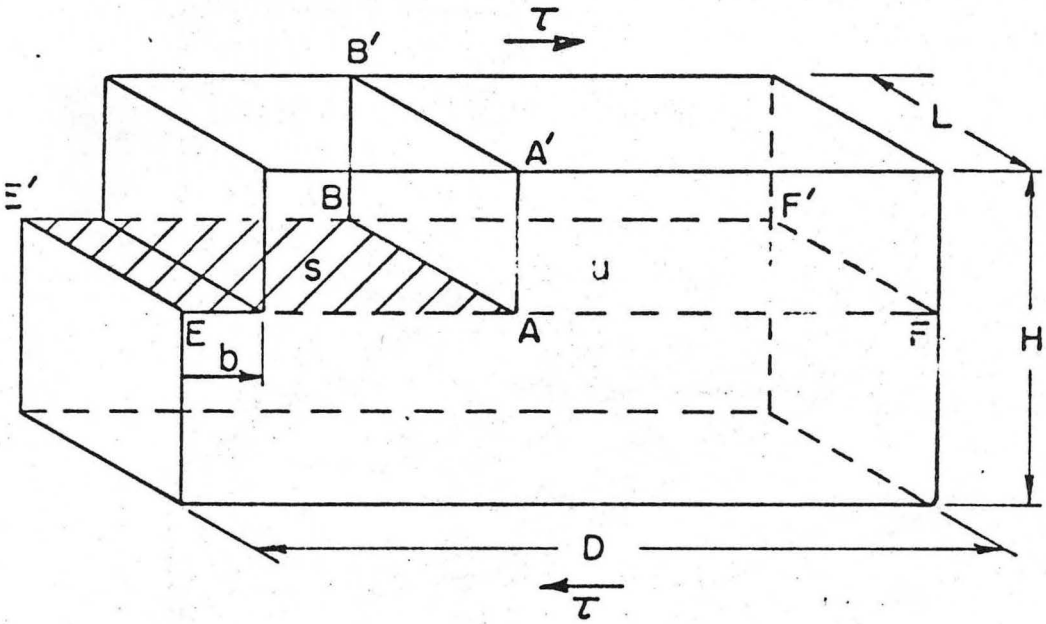

(a) EDGE DISLOCATION

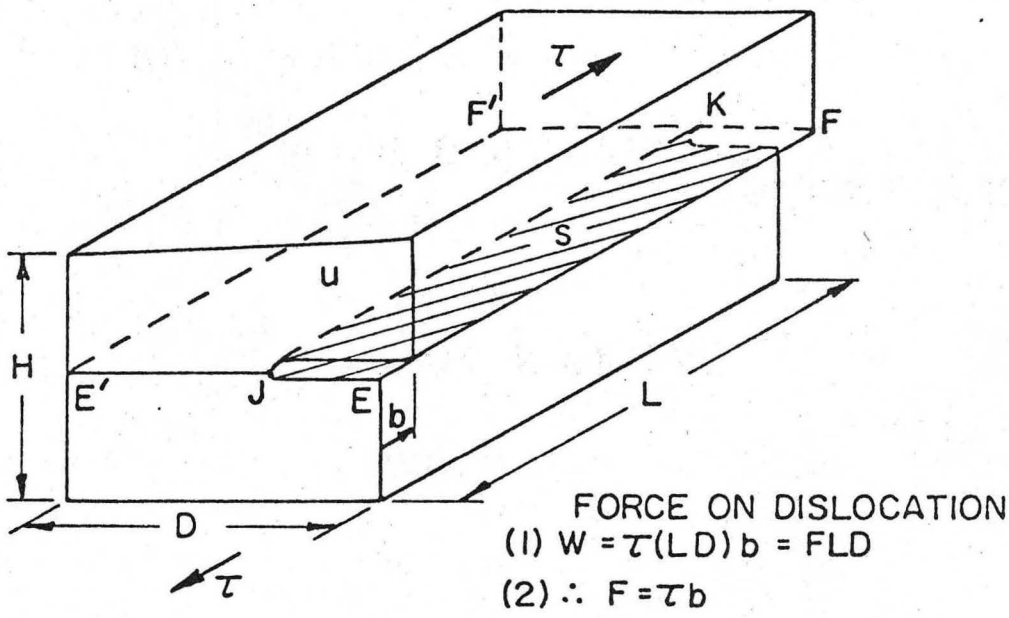

(b) SCREW DISLOCATION

GLIDE DISLOCATIONS

XBL717-7049

FIG. 2a, b

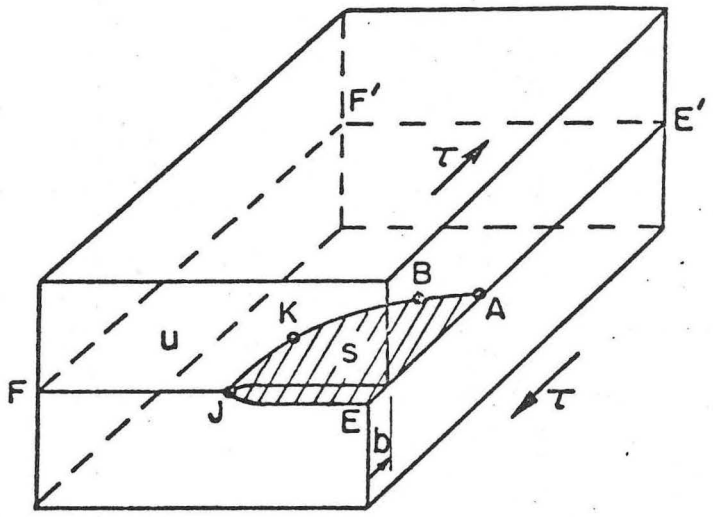

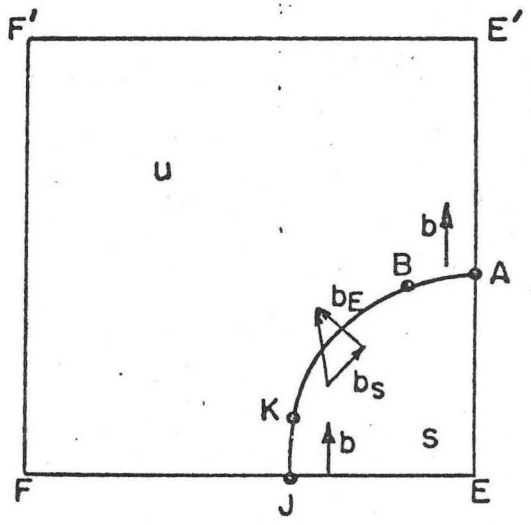

PLAN VIEW

(c) CURVED DISLOCATION

GLIDE DISLOCATION

XBL 717-7050

FIG. 2c

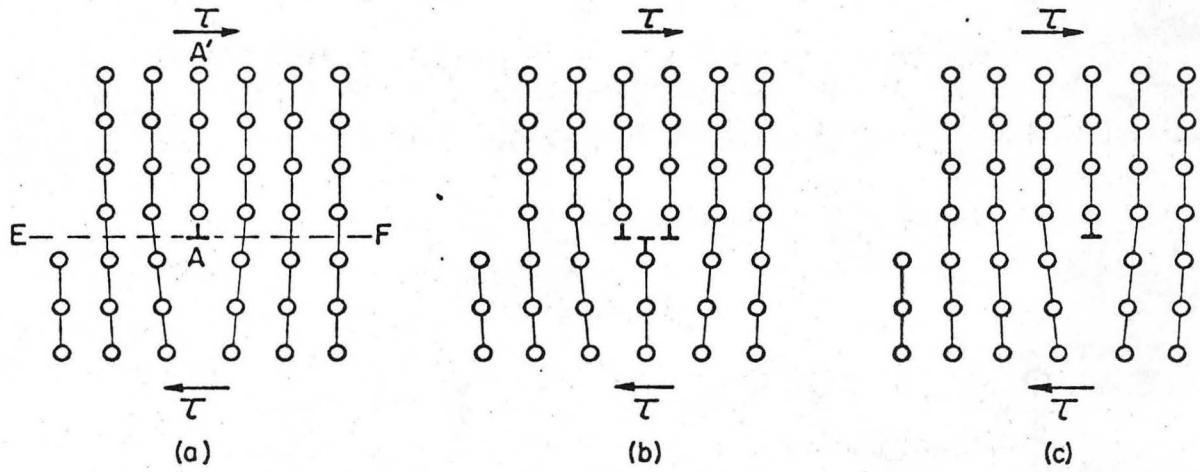

EDGE DISLOCATION

SLIPPING ONE BURGERS VECTOR

ATOMISTIC REPRESENTATION OF DISLOCATIONS

XBL717-7056

FIG. 3a, b, c

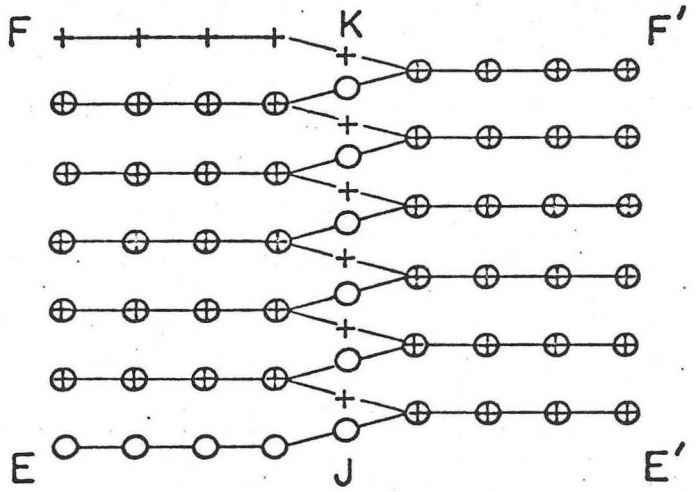

+ ATOMS ABOVE SLIP PLANE
O ATOMS BELOW SLIP PLANE

(d) PLAN VIEW OF SCREW DISLOCATION

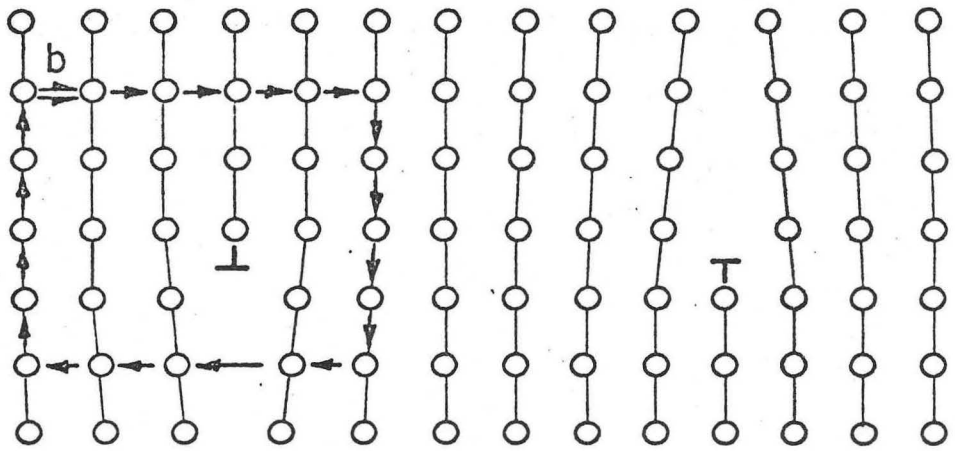

(e) POSITIVE AND NEGATIVE EDGE DISLOCATIONS

ATOMISTIC REPRESENTATION OF DISLOCATIONS

XBL 717-7057

FIG. 3d, e

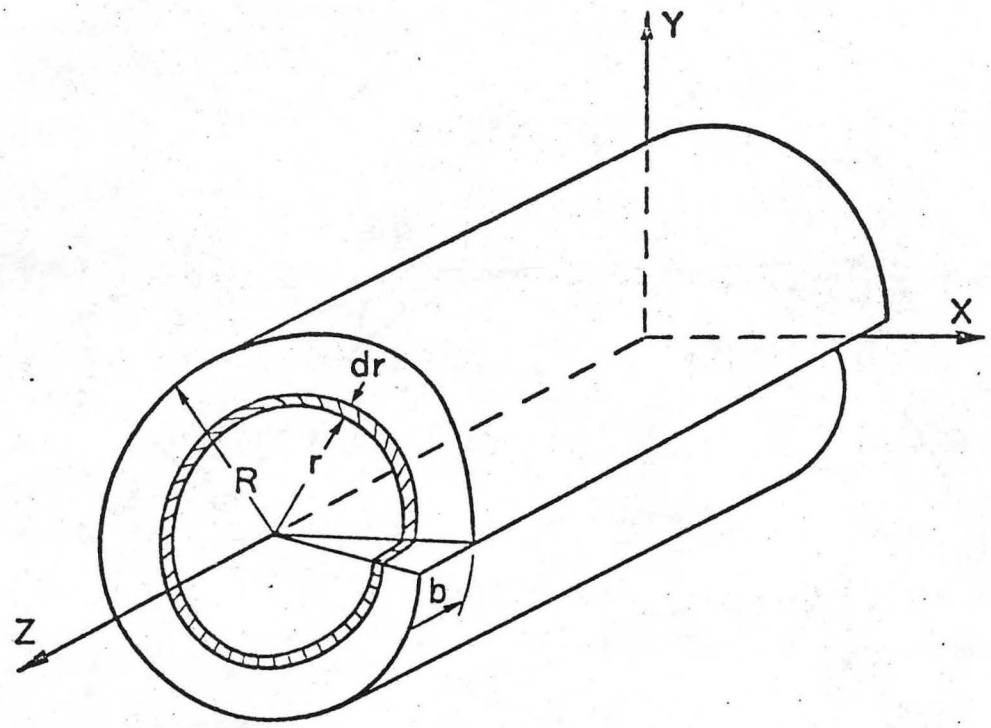

(3) $\gamma_E = b/2\pi r$

(4) $\tau = G\gamma_E = Gb/2\pi r$

(5) $\Gamma_s = \int_b^R 1/2\,\tau\,\gamma\,2\pi r\,dr + \Gamma_{sc}$

(6) $\Gamma_s = \frac{Gb^2}{4\pi} \ln R/b + \Gamma_{sc}$

(7) $\Gamma_s \approx Gb^2/2$

(8) $\Gamma_E \approx Gb^2/(1-\nu)2$

STRAIN ENERGY OF A SCREW DISLOCATION

XBL717-7051

FIG. 4

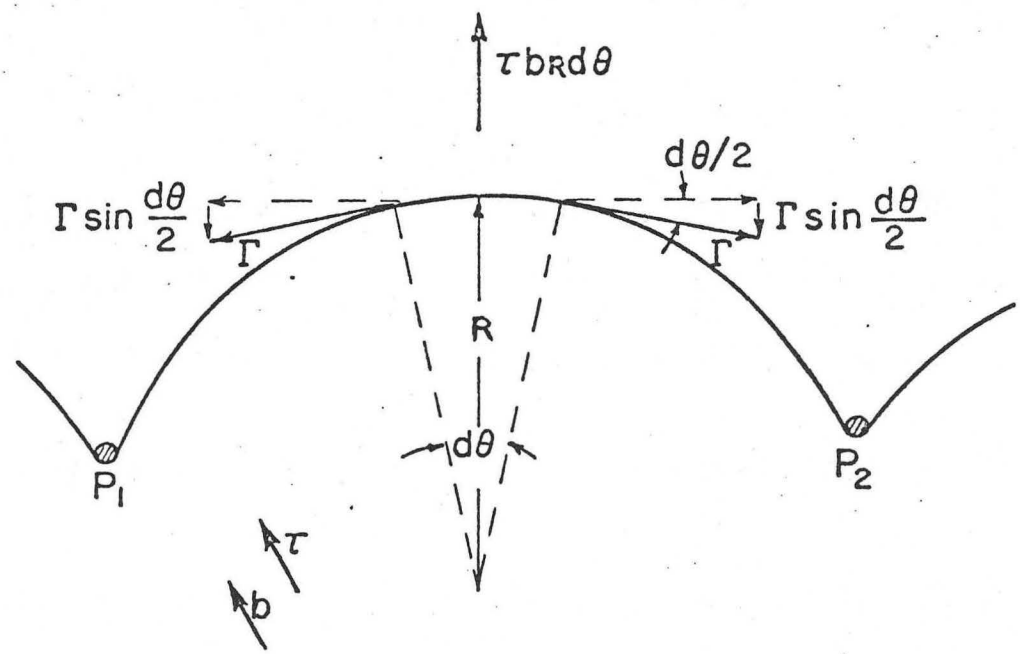

(9) $U_{DIS} = \ell \Gamma$

(10) $F = -\dfrac{\partial U_{DIS}}{\partial \ell} = -\Gamma$

(11) $\tau b R d\theta = 2\Gamma \sin \dfrac{d\theta}{2}$

(12) $\tau = \dfrac{\Gamma}{bR}$

RADIUS OF CURVATURE OF A DISLOCATION

XBL 717-7052

FIG. 5

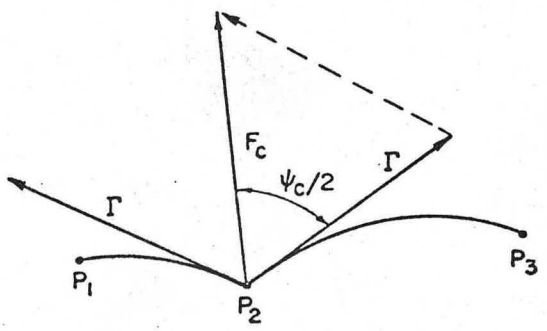

(a)

(13) $F_c = 2\Gamma \cos \psi_c/2$

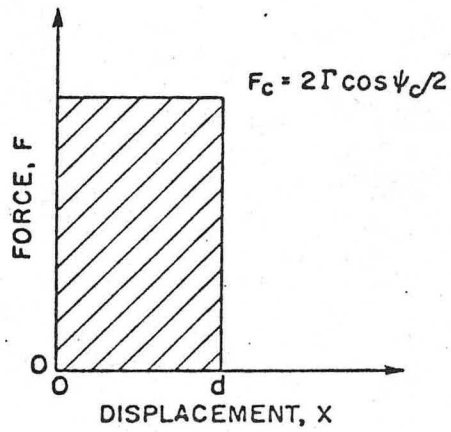

(b)

(14) WORK AT $0^\circ K = 2\Gamma d \cos \psi_c/2$

CUTTING POINT OBSTACLES

XBL717-7053

FIG. 6

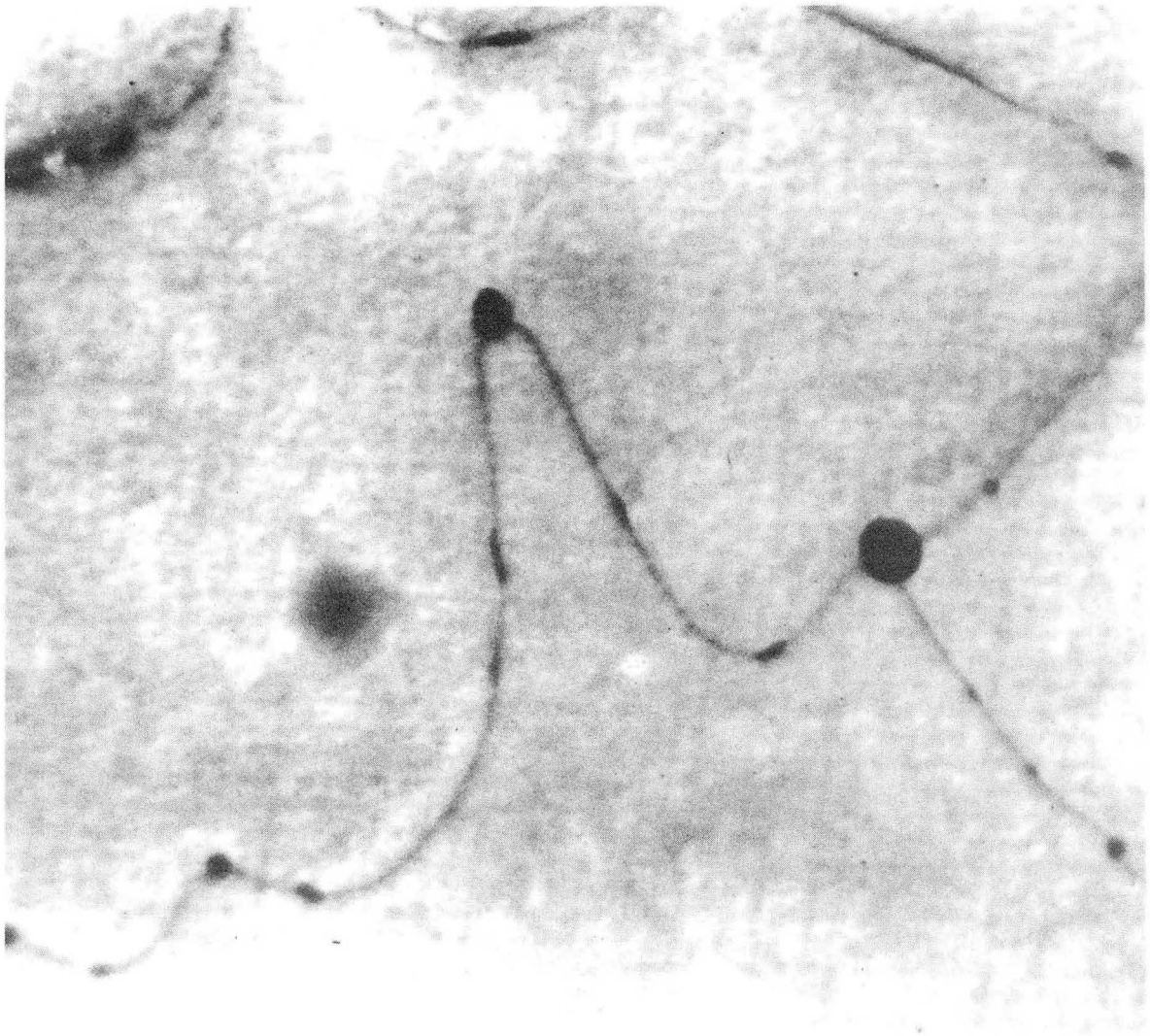

XBB 717-3342

Fig. 7

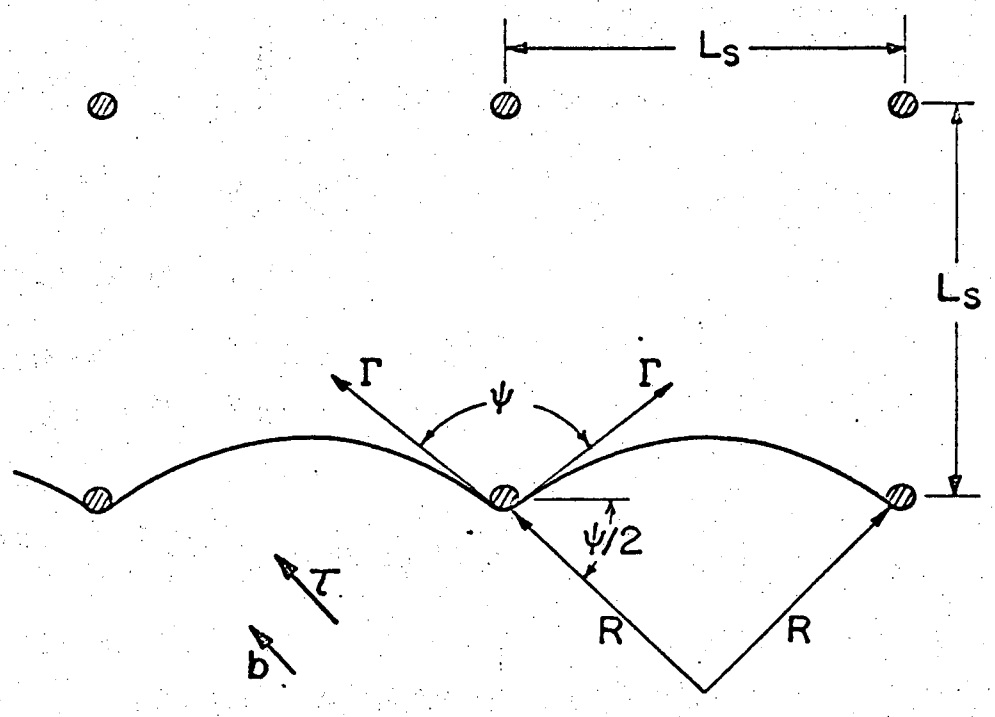

$$\tau = \Gamma/bR$$

$$L_s/2R = \cos \psi/2$$

WHEN

$$\psi = \psi_c$$

(15) $$\frac{\tau_0 L_s b}{2\Gamma} = \cos \psi_c/2$$

SQUARE ARRAY ANALYSIS

XBL717-7054

FIG. 8

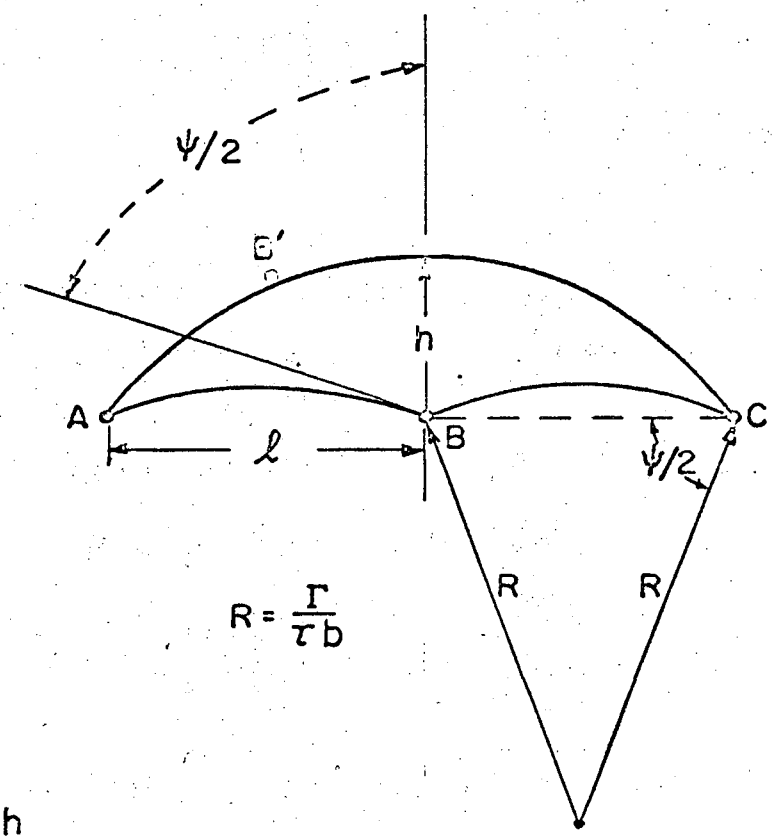

(16) $L_s^2 = \ell h$

(17) $R^2 = (R-h)^2 + \ell^2$

FOR $h \ll 2R$ (WEAK OBSTACLE ASSUMPTION)

$\ell^2 \approx 2Rh \approx 2R\ell_s^2/\ell$

(18) $\therefore \ell = L_s/(\tau L_s b/2\Gamma)^{1/3}$

AND

(19) $\cos\psi/2 = \ell/2R = \dfrac{\tau b \ell}{2\Gamma} = \left(\dfrac{\tau L_s b}{2\Gamma}\right)^{2/3}$

ALSO

(20) $h = L_s^2/\ell = L_s\left(\dfrac{\tau L_s b}{2\Gamma}\right)^{1/3}$

FRIEDEL'S ANALYSIS

XBL 717-7055

FIG. 9

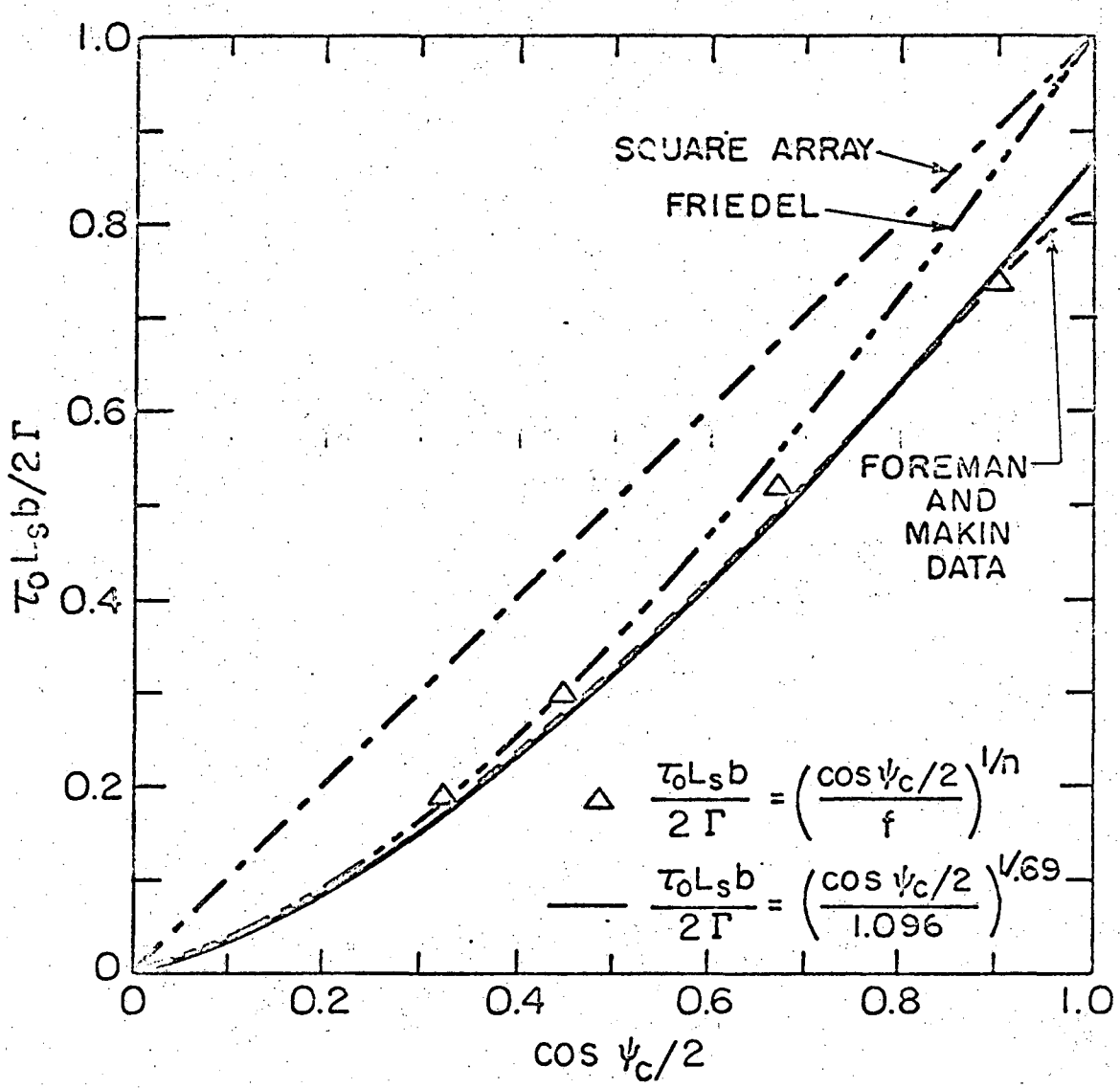

XBL717-7060

FIG. 10

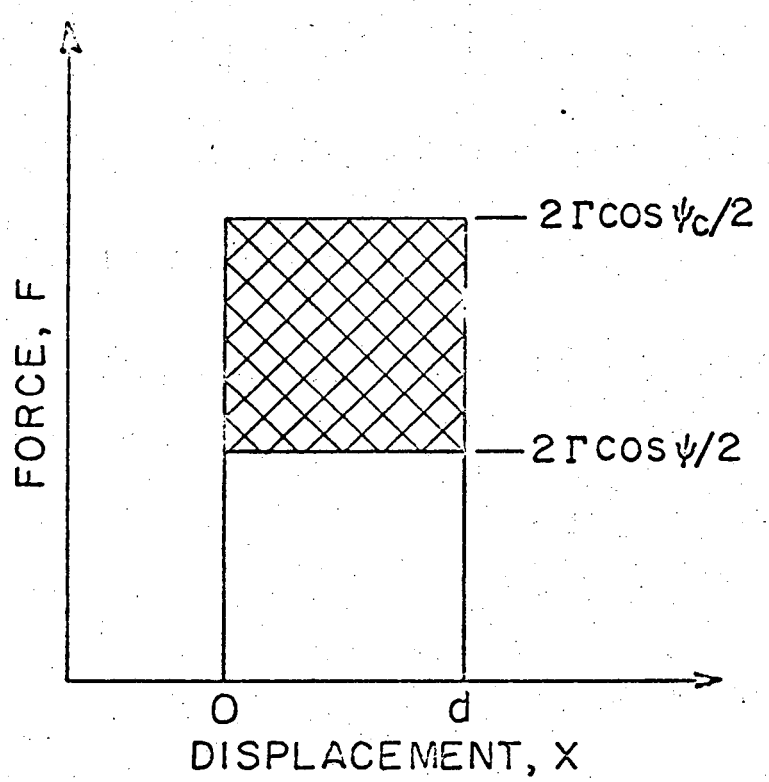

$$g = 2\Gamma d\,(\cos\psi_c/2 - \cos\psi/2)$$

RECTANGULAR FORCE-DISPLACEMENT DIAGRAM

XBL 717-7064

FIG. 11

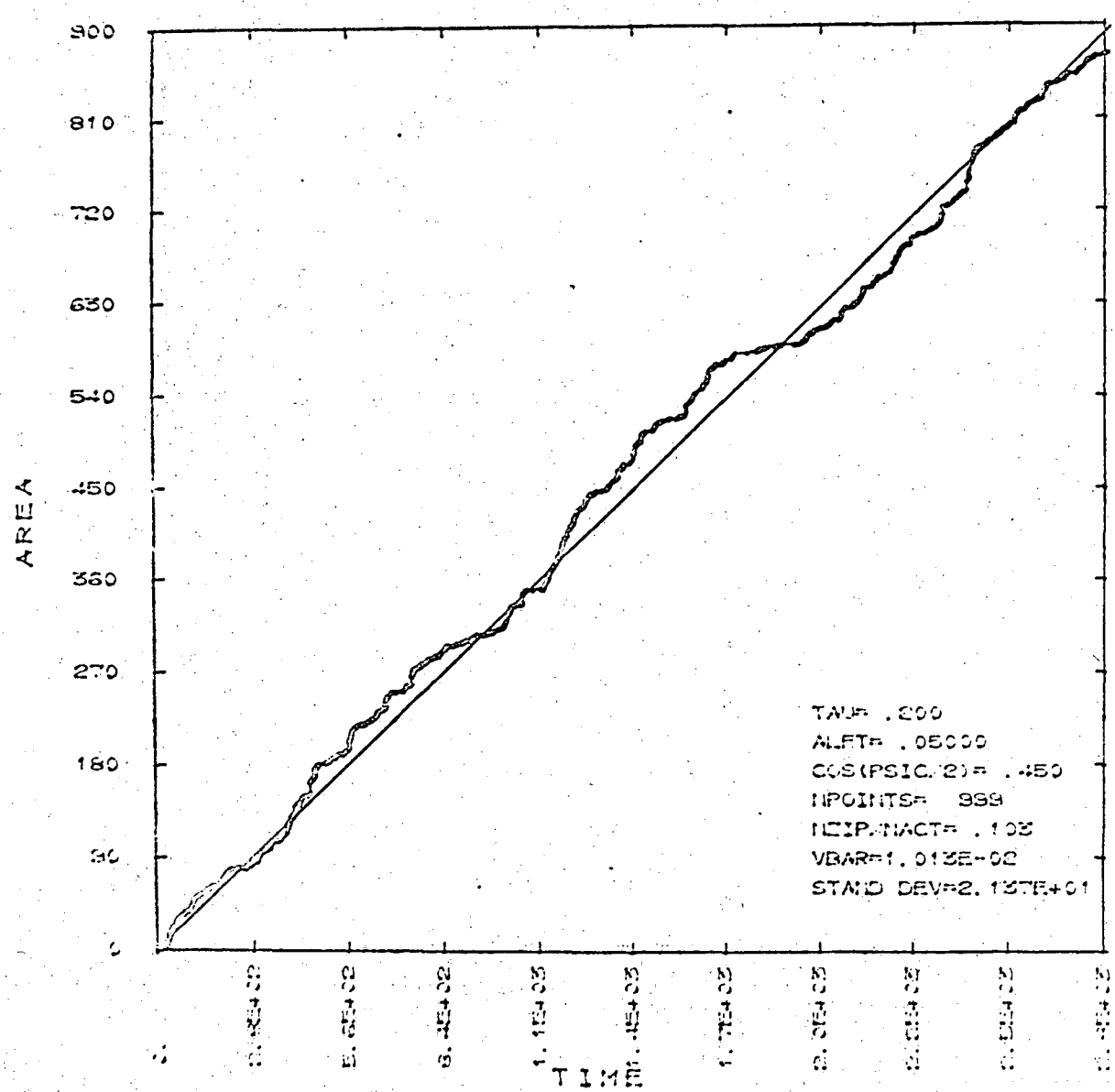

XBL 717-1203

FIG. 12

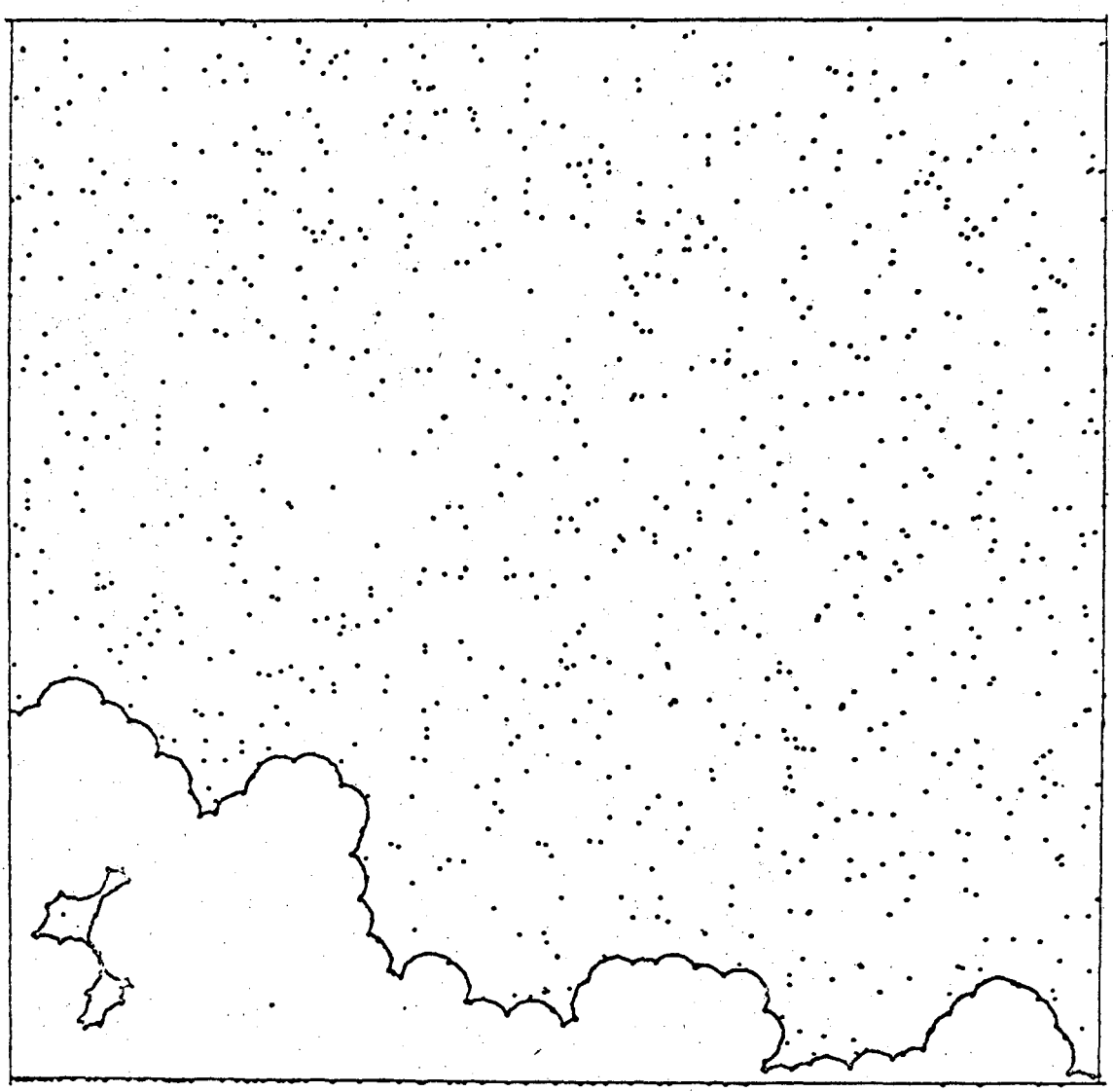

XBL 717-1205

FIG. 13

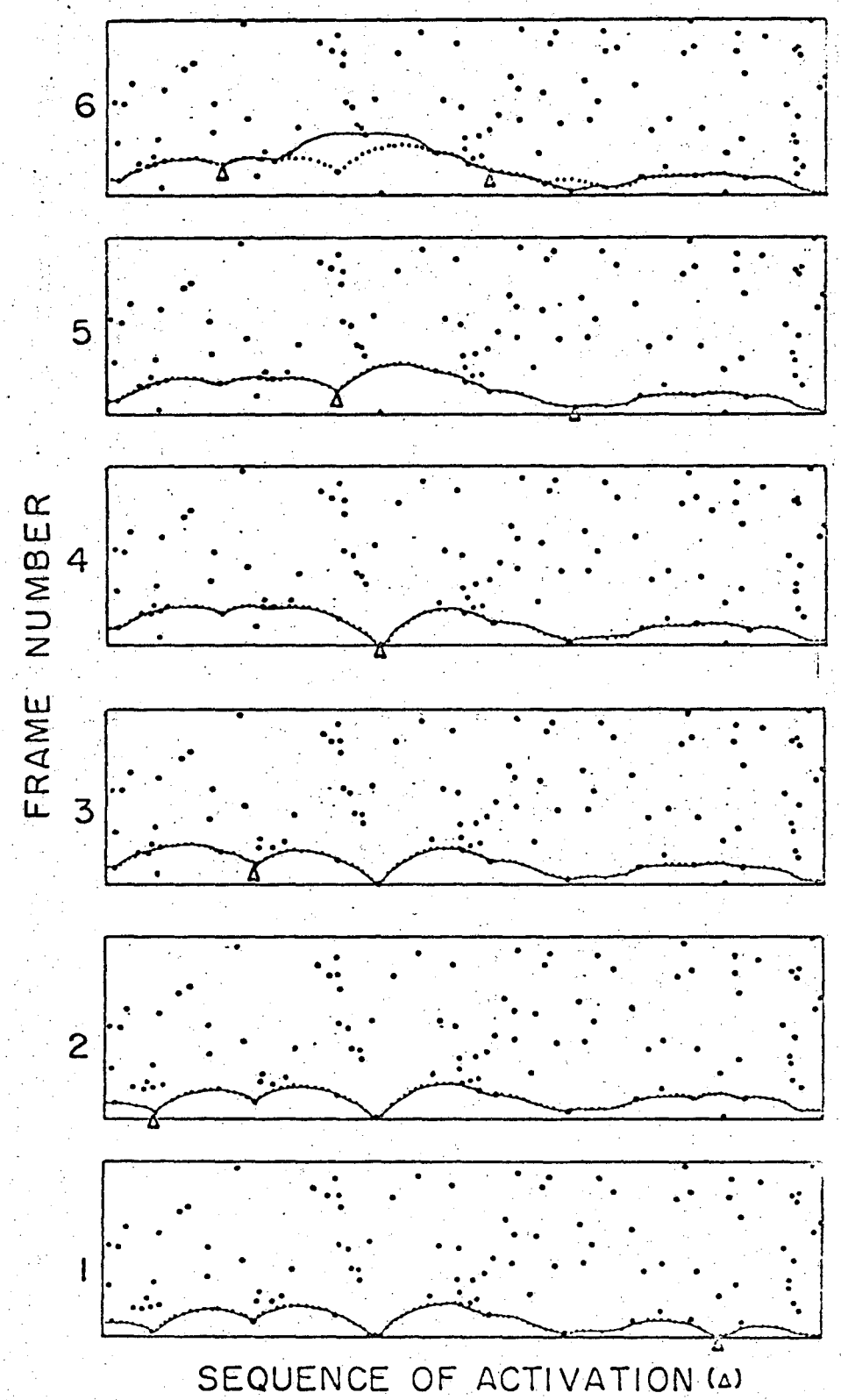

XBL717-7067

FIG. 14

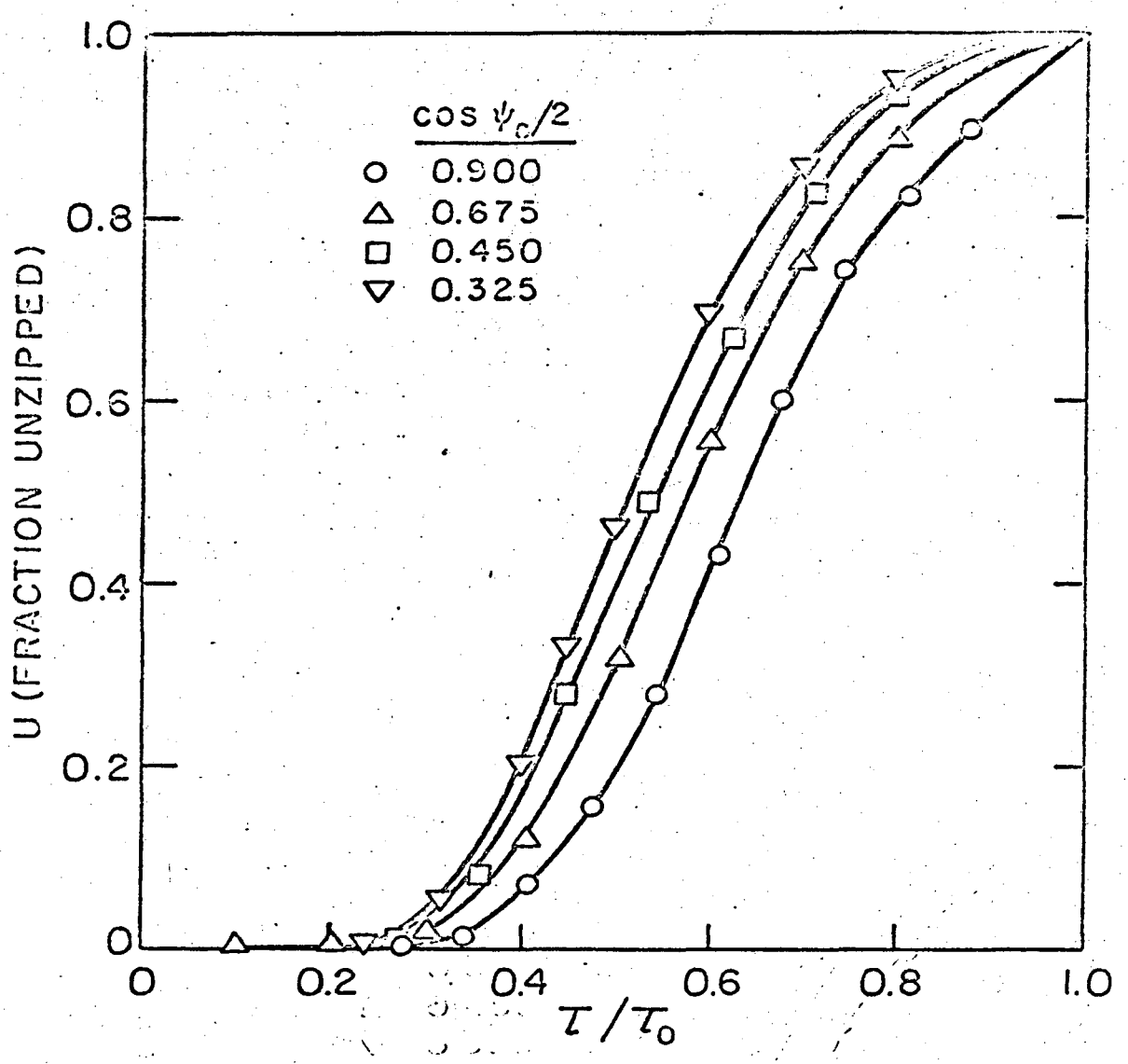

XBL717-7066

FIG. 15

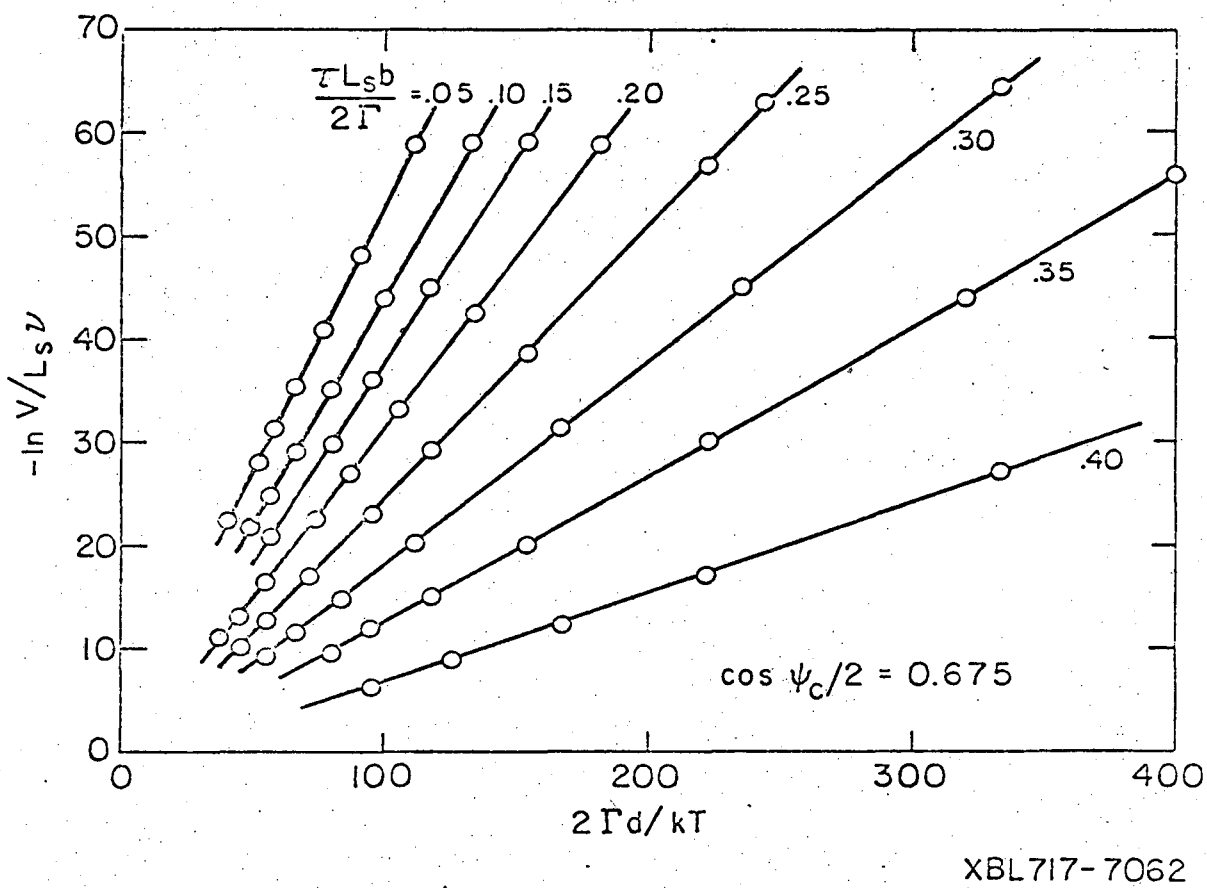
$\frac{\tau L_s b}{2\Gamma}$ = .05 .10 .15 .20 .25 .30 .35 .40
cos $\psi_c/2$ = 0.675
$-\ln V/L_s\nu$
$2\Gamma d/kT$
0
10
20
30
40
50
60
70
100
200
300
400
XBL717-7062

FIG. 16

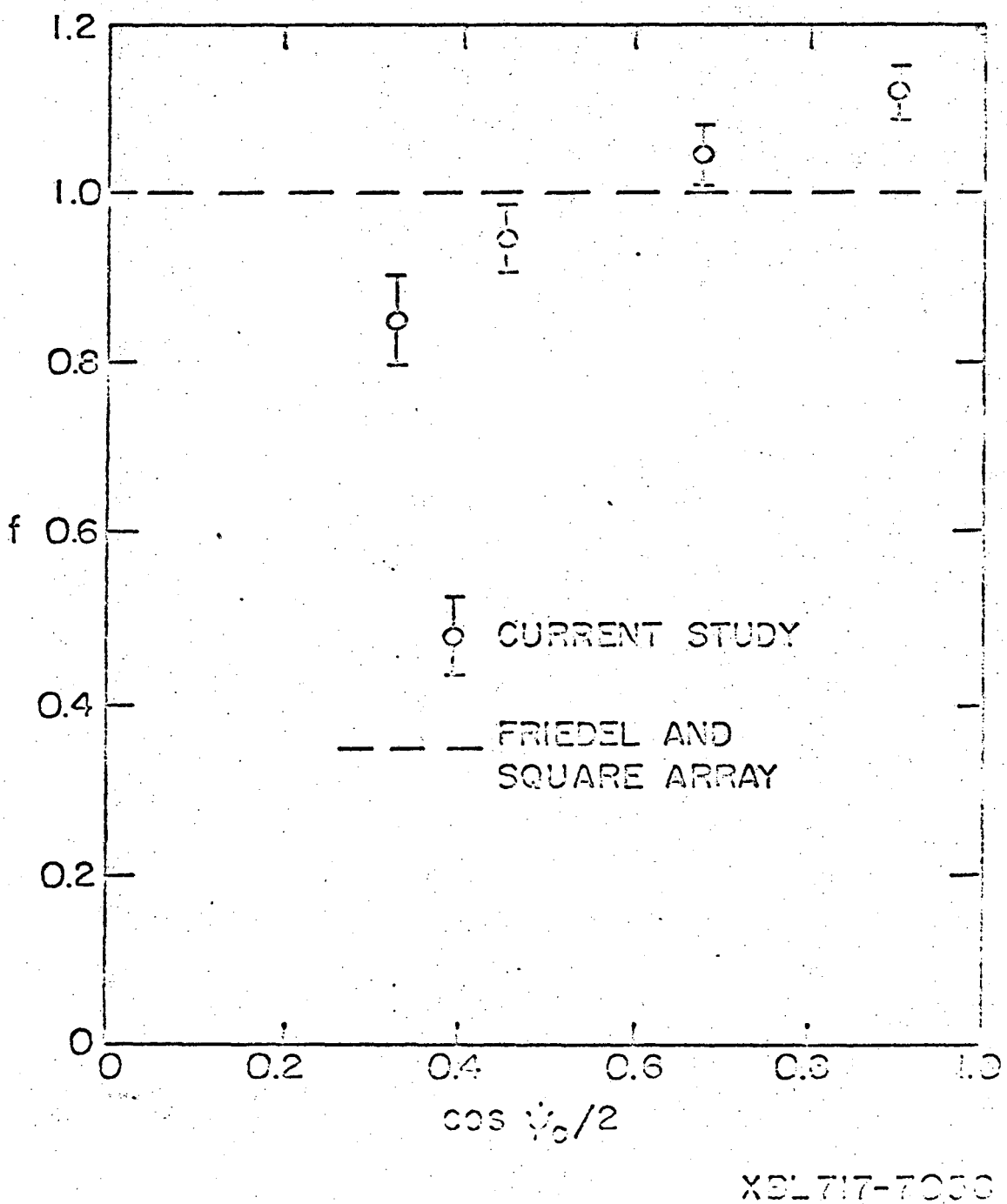
1.2
1.0
0.8
f 0.6
0.4
0.2
0
0
0.2
0.4
0.6
0.8
1.0
cos $\psi_0/2$
CURRENT STUDY
FRIEDEL AND
SQUARE ARRAY
XBL717-7000

FIG. 17

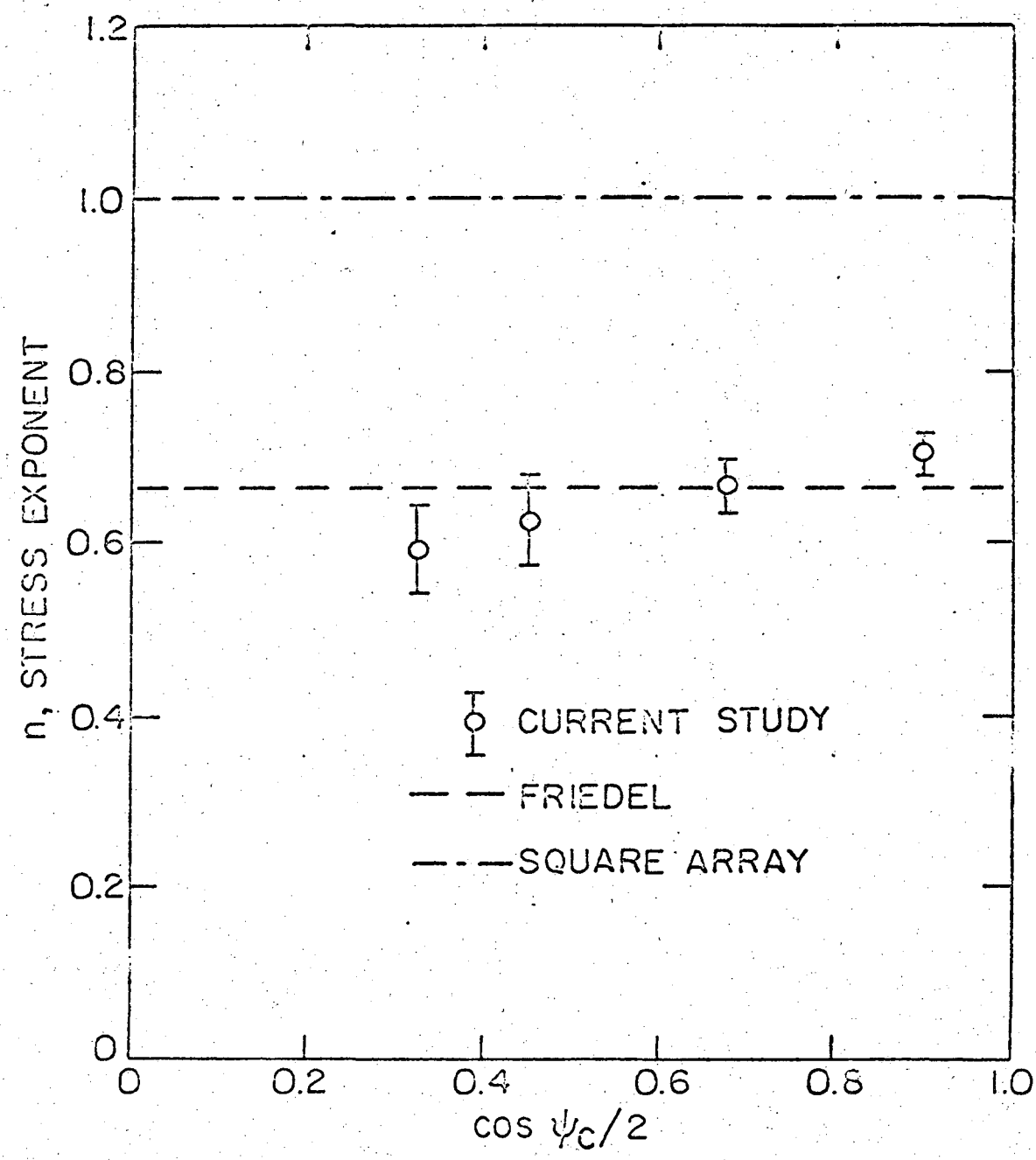

XBL717-7059

FIG. 18

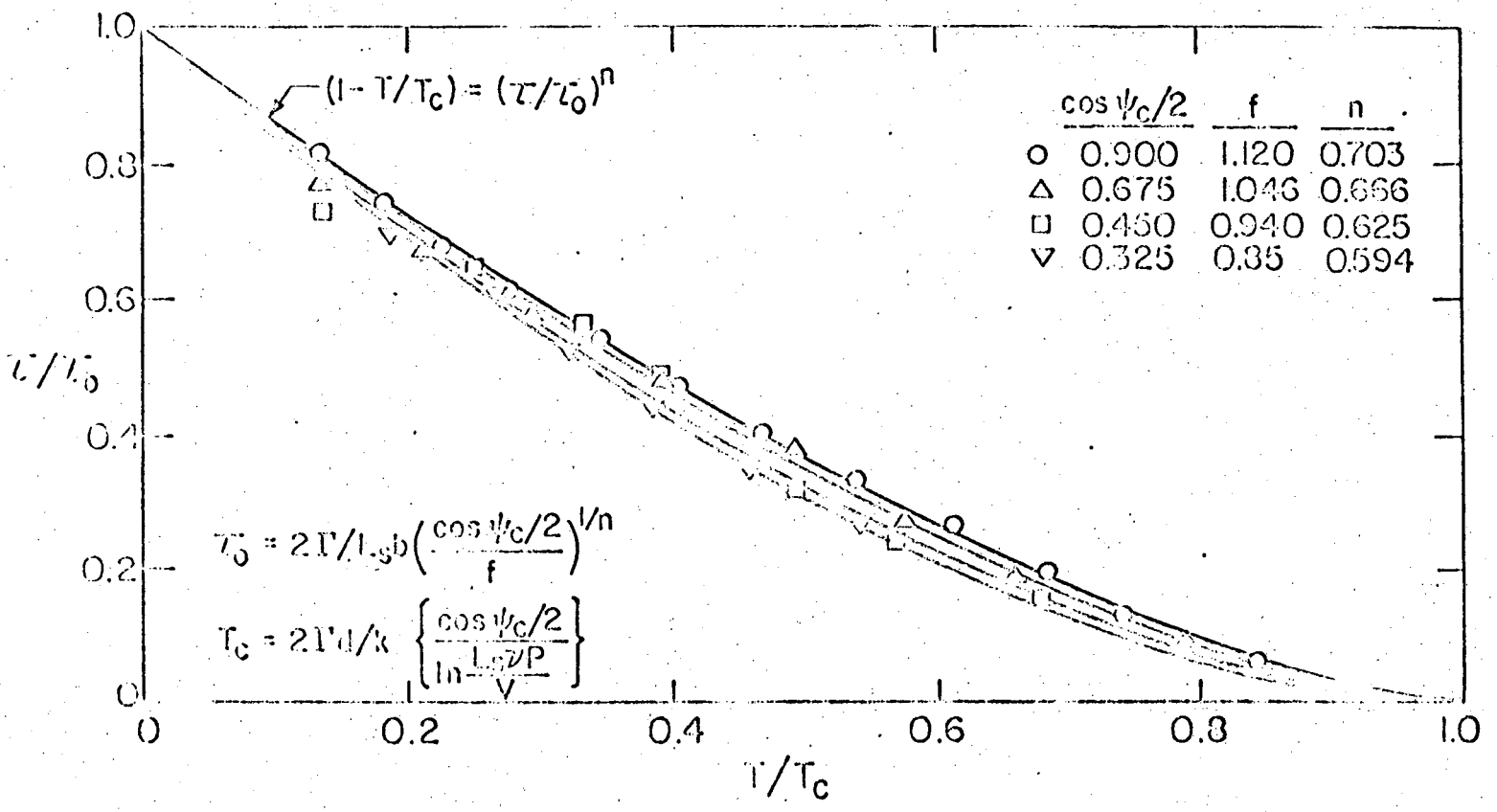

XBL717-7063

FIG. 10

References

1. G. I. Taylor, Proc. Roy. Soc. A145, 362 (1934).

2. E. Orowan, Zeit. Phys. 89, 605, 614, 634 (1934).

3. M. Polanyi, Zeit. Phys. 89, 660 (1934).

4. P. B. Hirsch, R. W. Horne, and M. J. Whelan, Phil. Mag. 1, 677 (1956).

5. W. Bollmann, Phys. Rev. 103, 1588 (1956).

6. A. H. Cottrell "Dislocations and Plastic Flow in Crystals", Oxford at the Clarenden Press (1953).

7. W. T. Read, Jr., "Dislocations in Crystals", McGraw-Hill Book Co. New York (1953).

8. M. Cohen Ed. IMD Seminar on "Dislocations in Metals", Amer. Inst. Min. and Met. Engrs. New York (1954).

9. J. Weertman and J. R. Weertman, "Elementary Dislocations Theory", The Macmillan Co., New York (1963).

10. J. Friedel "Dislocations" Addison-Wesley Publish. Co., Reading, Mass. (1964).

11. A. Rosenfield, G. T. Hahn, A. L. Bement, Jr., R. I. Jaffee Eds., "Dislocation Dynamics", McGraw-Hill Book Co., New York (1968).

12. J. P. Hirth and J. Lothe, "Theory of Dislocations", McGraw-Hill Book Co. New York (1968).

13. F. R. N. Nabarro "Theory of Crystal Dislocations", Oxford Univ. Press, Oxford (1967).

14. J. A. Simmons and R. Bullough, Editors "Fundamental Aspects of Dislocation Theory" Nat. Bu. Std. Special Publication 317, Vols. I and II Washington D.C. (1970).

15. J. E. Dorn "Low-Temperature Dislocation Mechanisms in Dislocation Dynamics" McGraw-Hill Book Co., p. 27 (1968).

16. J. E. Bird, A. K. Mukherjee and J. E. Dorn, "Correlations Between High-Temperature Creep and Structure in Quantitative Relation Between Properties and Microstructure" Israel University Press, Haifa, p. 255 (1969).

17. D. Klahn, A. K. Mukherjee and J. E. Dorn "Strain Rate Effects", Second International Conf. on Strength of Metals and Alloys" Amer. Soc. for Met. p. 951 (1970).

18. G. Thomas, "Transmission Electron Microscopy of Metals", John Wiley & Sons, Inc., pp. 225 (1962).

19. J. Friedel "Dislocations", Pergamon Press, Oxford, p. 224 (1964).

20. A. J. E. Foreman and M. J. Makin, Phil. Mag., 14, 911 (1966).

21. A. J. E. Foreman and M. J. Makin, Canad. J. Phy. 45, 511 (1967).

22. S. Glasstone, K. S. Laidler, and H. Eyring, "The Theory of Rate Processes", McGraw-Hill Co., New York, (1941).

23. A. V. Granato, K. Lücke, J. Schlipf and L. S. Teutonico, J. Appl. Phys., 35, 2732 (1964).

24. See ref. 14, p. 1112.

25. See ref. 14, p. 1034.

26. U. F. Kocks, Phil. Mag. 13, 541 (1966).

27. U. F. Kocks, Canad. J. Phys., 45, 731 (1967).

28. U. F. Kocks, Proc. Int'l. Conf. on Strength of Metals and Alloys, Trans. Jap. Inst. Met., 9 (Suppl.), 1 (1968).

29. U. F. Kocks, "Physics of Strength and Plasticity", ed. A. Argon, M.I.T. Press, p. 143, (1969).

30. See ref. 14, p. 1077.

31. See ref. 14, p. 1065.

32. W. Frank, Phy. Stat. Sol. 26, 197 (1968).

33. R. Labusch, Phy. Stat. Sol. 41, 659 (1970).

APPENDIX

A computer generated movie, "Dislocation Motion Through a Random Array of Point Obstacles," was produced using the CDC 6600 Vista System. The three significant experimental parameters, expressed in dimensionless units, i.e., temperature ($2\Gamma d/kT$), applied stress (τ/τ_o), and relative obstacle strength, ($\cos \psi_c/2$), were varied to illustrate the following phenomena:

(1) At low stress levels ($\tau/\tau_o < 0.5$) the dislocation remains relatively straight and moves in a point by point fashion through the array. The dislocation velocity increases through regions of low obstacle density and slows down in regions where obstacles are closer together than the average separation.

(2) At higher stresses ($\tau/\tau_o > 0.5$), when a particular obstacle is passed by thermal activiation, the force on adjacent obstacles often exceeds the obstacle resistance and they are cut instantaneously. They are "unzipped."

(3) In general, for different values of the temperature parameter, $2\Gamma d/kT$, the activation sequence was different. This is illustrated by superposition of the jumping sequences of two dislocations at different values of $2\Gamma d/kT$.

(4) For high stresses ($\tau/\tau_o > 0.8$) and strong obstacles ($\cos \psi_c/2 \simeq 1$) the dislocation assumes a configuration analogous to cumulus clouds, penetrating the array deeply along paths of easy movement (low obstacle densities). Dense obstacle groups are often encircled by the dislocation and closed loops left behind when positive and negative branches of the dislocation meet and annihilate. These loops collapse and disappear with time by thermal activation and self-annihilation.

LEGAL NOTICE

This report was prepared as an account of work sponsored by the United States Government. Neither the United States nor the United States Atomic Energy Commission, nor any of their employees, nor any of their contractors, subcontractors, or their employees, makes any warranty, express or implied, or assumes any legal liability or responsibility for the accuracy, completeness or usefulness of any information, apparatus, product or process disclosed, or represents that its use would not infringe privately owned rights.

TECHNICAL INFORMATION DIVISION
LAWRENCE RADIATION LABORATORY
UNIVERSITY OF CALIFORNIA
BERKELEY, CALIFORNIA 94720